CLAS-NOTE-2001-009

e/π Rejection in CLAS

M. V. Kossov
ITEP, Moscow

May 14, 2001

Abstract

In the paper the e/π rejection algorithm is developed and tested on the $e^-p \to e^-\pi^+\pi^-p$ ($e^-p \to e^-e^+e^-p$) reactions measured in the e1c run at the detector CLAS. About $2{\cdot}10^5$ events of that topology have been selected and the energy-momentum conservation has been tested for each reaction. The developed functional criterion, taking into account β of the particle (calculated on the basis of the time-of-flight and the track length), its momentum p, the energy deposited in the Electromagnetic Calorimeter E, and the signal from the Cerenkov Counter, separated only 10 "$e^-e^+e^-$" events out of the total sample, 9 of these events were identified as the e^+e^- Dalitz pairs and only one event was found to be a candidate to the decay of the ρ meson in an electron and a positron. The $5{\cdot}10^{-6}$ ratio corresponds to the expectation according to the branching ratios for the ρ meson (taking into account the dominant contribution of the $\Delta\pi$ final states).

1 Introduction

The main goal of the paper is to show that it is possible to suppress $\pi^+\pi^-$ pairs in CLAS and at the same time to keep the efficiency for the e^+e^- pairs high enough. This is necessary for the $g7$ run time measurements, where the e^+e^- pairs are included in the trigger and the rest of the $\pi^+\pi^-$ decays should be separated from the e^+e^- decays of the vector mesons off-line.

About one million of the cooked $e^-p- > e^-\pi^+\pi^-(p)(\gamma)(\gamma)$ events from the $e1c$ run (with E_e=2.57 GeV, I_{torus}=1500 A) have been selected (π^- meson means just the second negative relativistic particle, so it includes electrons; no positrons were found at the cooking level for this reaction; particles in brackets are optional). The initial energy of electrons matches the energy of the energy of electrons in $g7$ run (E_e=2.4 GeV). Any of the three final relativistic particles can be an electron (positron) or pion, nevertheless in the paper they are named "e^-", "π^+" (pos), and "π^-" (neg) correspondingly. The low magnetic field helps to increase the CLAS acceptance for the positive particles. At the first attempt a half of the selected events contained "ghosts" of the negative particles. In the events with such a "ghost" both negative particles had the same EC (Electromagnetic Calorimeter) signal, the same SC (Scintillation Counters) time and ID (a sector number and a counter number), but different DC (Drift Chamber) momentum and the path length from the reaction vertex to SC. Such events have been filtered out and did not come to the selected million of events.

In the paper the following definitions are used:

1. a number of events in a bin of any histogram is always logarithmic;
2. all effective and missing masses are plotted as a squared values;
3. $name_{BANK}$ means the variable "name" from the BOS bank "BANK".
4. c=1.

2 Timing in CLAS

The main algorithm of the time-of-flight (TOF) reconstruction in cooking for the electron beam in CLAS includes the following steps:

1. Match the DC tracks with SC, CC (Cerenkov Counter), and EC signals;

2. Using EC (and sometimes CC) signal select "the electron" (if there are a few negative candidates, select higher momentum from DC);

3. Trace back "the electron" from SC to the reaction vertex along the DC path ($L_e = time_{SCPB}$) and get the vertex time $t_V = t_{SC} - L_e$ (as for an electron β=1; $t_{SC} = path_{SCPB}$);

4. Attract the t_V to the nearest RF bunch and get $t_{RF} = stt_{HEVT}$ time as a start time for all timing (then the $t_e = t_{SC} - t_{RF}$ and $\beta_e \neq 1$).

5. The problem is that the path length from the CEBAF accelerator to the CLAS detector can be different for the different beam tuning, so the "RF timing" itself must be calibrated from run to run, using the CLAS timing. That is why after each beam tuning the new run should be started.

6. If there is a SC counter with a bad resolution or bad calibration or a soft negative pion is misidentified as an electron, then the shift from the RF bunch in time can be more than 1 ns and the CLAS timing attracts the measured t_V value to the wrong RF bunch time (which makes 2 ns uncertainty in timing of the particular event). The probability of such events is relatively low but anyway this problem can be partially cured using the EC time.

7. In the $g7$ run the situation with timing is much better as there are two (not one) relativistic particle in the trigger and the RF bunch is secured by the two t_{SC} measurements and in addition by the tagger timing.

In the analysis the time difference in the vertex point is defined as $d_j^i = t_j - \frac{L_j}{p_j}\sqrt{p_j^2 + m_i^2}$, where t and L are defined above and $p = pmom_{EVNT}$ is a momentum measured in DC; the index i stands for the different

hypothesis about the mass of the relativistic particle, so m_i equals to m_e or m_π; index j stands for "e", "pos", and "neg". The $d_e^e(d_e^\pi)$ distribution is shown in Fig. 1.

In addition to the clear maximum at d_e^e=0, there is a small maximum at d_e^π=0 and even some indication on a maximum at (d_e^e=-1, d_e^π=-2). The "$Nent$" value on the picture shows the total number of the collected events. Just to finish with the electron timing in Fig.2 the same plot is shown for the events with the trigger cut, which is described below (it demands EC and CC signals for all three relativistic particles).

On this plot the maxima at $d_e^e = 0.8$ and at ($d_e^e = 0.8$, d_e^π=0.8) can be seen. These maxima correspond to the mentioned above possibility to get the wrong RF bunch. The d-distribution of such events drops from $d = \pm 1$ to $d = 0$. This proves the specific timing cut for the scattered electrons: $d_e^e > -0.5$ AND $d_e^\pi < 0.5$. Comparing the numbers of the events from the two pictures it is possible to estimate that the trigger suppression for the $\pi^+\pi^-$ events is about 10^{-3}.

The similar plot is shown in Fig. 3 for the second negative relativistic particle ("neg"). A lot of the "near bunch" events can be seen on the picture what proves the general timing cut $|d^e| < 1$ AND $|d^\pi| < 1$ for all three relativistic particles.

In Fig.4 the similar plot is shown for the positive relativistic particle ("pos"). It is important to point out that there is almost no maximum for the $d_e^e = 0$, which means that the contamination of the positrons is really small.

So the resulting timing cut ("silver" cut) is defined as $|d^e| < 1$ AND $|d^\pi| < 1$ for all three relativistic particles and in addition for the first negative relativistic particle $d_e^e > -0.5$ AND $d_e^\pi < 0.5$. After this cut the D-selector (DS-factor) can be defined as $DS = |d^e + 0.5| - |d^\pi - 0.5|$. The DS-factor is strongly correlated with the calculated $\beta = \frac{L}{t}$ for the relativistic particles. The $\beta(DS)$ plot is shown in Fig. 5 for all three relativistic particles together, so to recover the number of events which pass through the "silver" cut, the number of events shown on the picture should be divided by 3. That is only 73% of the events pass the "silver" cut. It should be noted that only in case of ideal measurements the $beta$ and the DS factor are duplicating each other. For the final resolution they give two projections of the (v,p) distribution and are complementary.

The T-selector (TS-factor) is defined as $TS = 8 \cdot \beta - DS$. The distribution over DS-factor is shown in Fig. 6.

3 The Dalitz e^+e^- pairs and the $\pi^+\pi^-/e^+e^-$ rejection task.

The TS-factor helps to make "100%" separation of electrons and pions for the momenta below 0.2 GeV. The TS(p) plot is shown in Fig. 7. So the π/e rejection task can be considered to be solved for this range of momentum (energy). On the other hand in $g7$ run we are not interested in so soft electrons (positrons) to be accepted as they only increase the low effective mass background and do not add any acceptance for the vector mesons.

The third reason why the relativistic particles with energy less than 0.2 GeV should be cut out in the task of the π/e rejection is because there are a lot of the Dalitz e^+e^- pairs, which form an unnecessary background. The effective mass distribution for the soft e^+e^- pairs is shown in Fig. 8. Any of the e-pos or the neg-pos pairs, when both the electron and the positron have p<0.2 GeV and TS>8, is plotted. If both e-pos and the neg-pos pairs come through this cut then the minimum mass value is plotted. Almost all effective masses are below .005. The rest of the distribution can be explained as a secondary scattering/interaction of the electrons and positrons. This hypothesis is indirectly confirmed by the zero effective mass of the $e^+e^-\gamma$ combinations, plotted on the next figure.

The distribution over the effective mass of the $e^+e^-\gamma$ system with the condition $m^2_{e^+e^-}$<.01 is plotted in Fig. 9. In addition to the π_0 signal (shifted to the higher masses because of the secondary interactions of the charged particles) the clear maximum at low effective masses is seen. These are the events when the

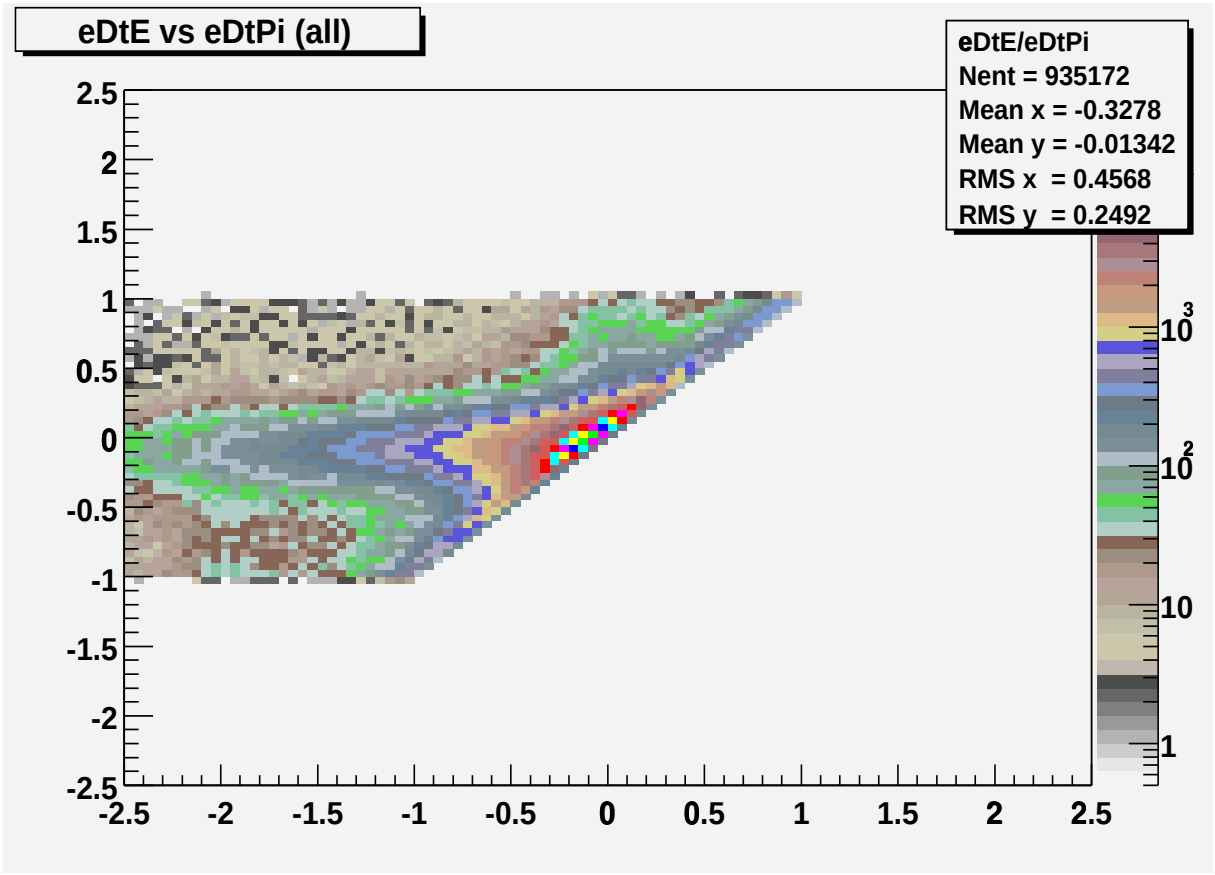

Figure 1: The time difference in the vertex point (two possible masses) for the scattered electron (see text).

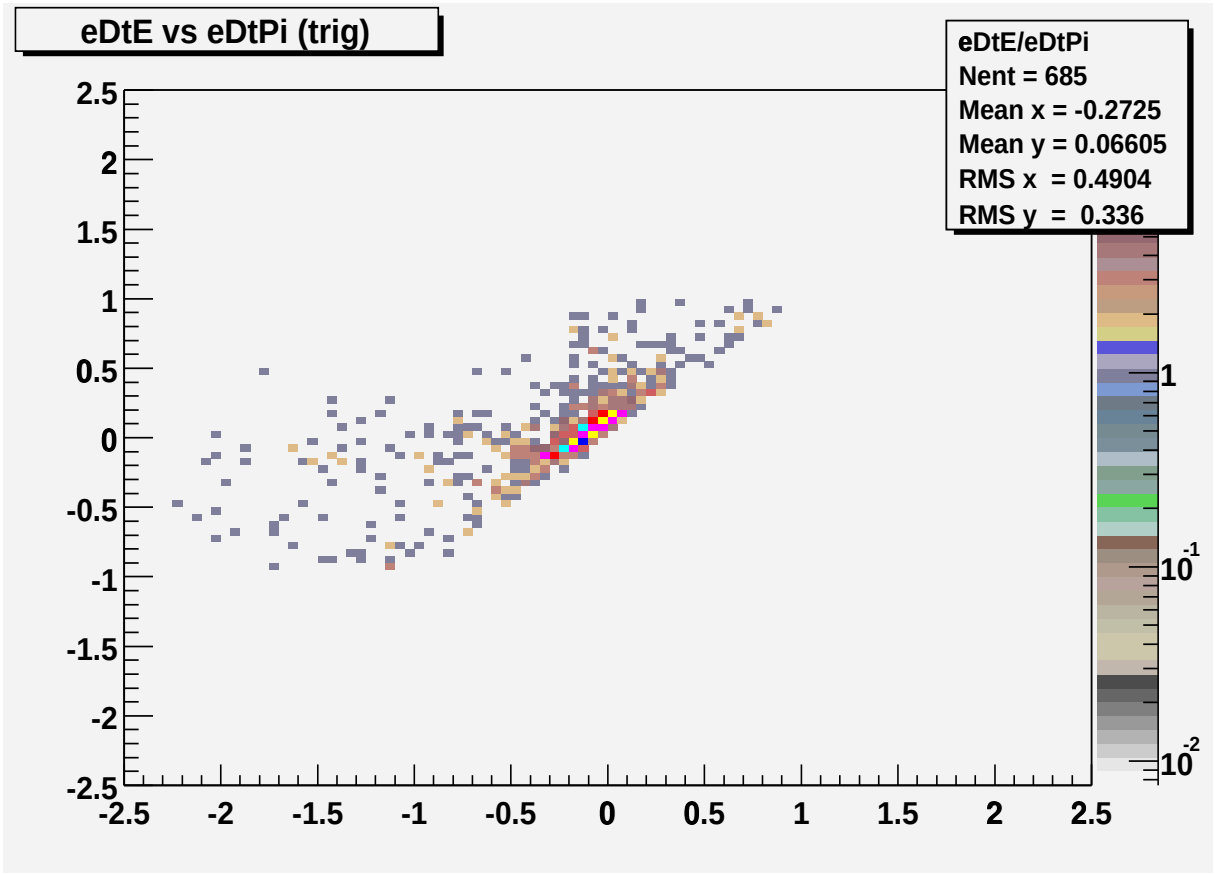

Figure 2: The same as in Fig. 1, but for the events with the trigger cut (not including timing cut).

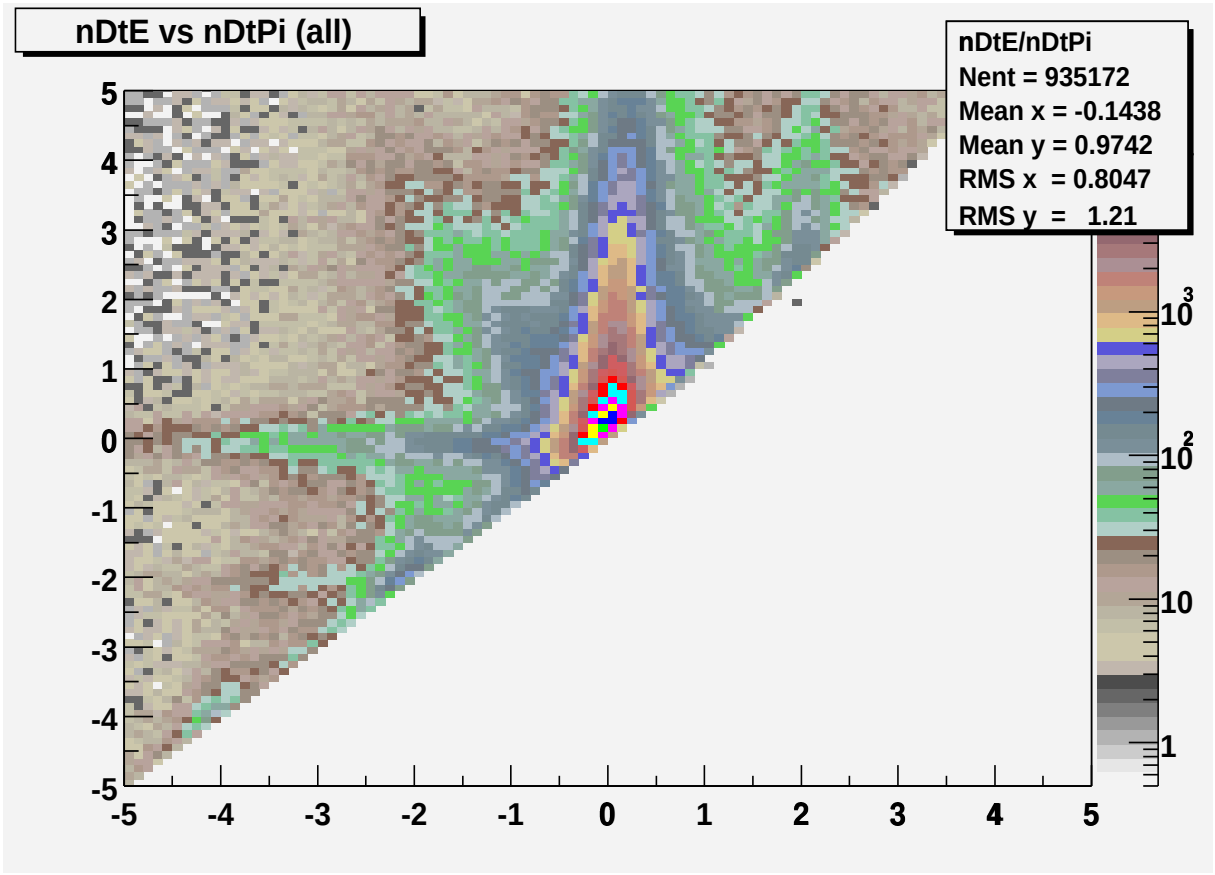

Figure 3: The same as in Fig. 1, but for the second negative relativistic particle.

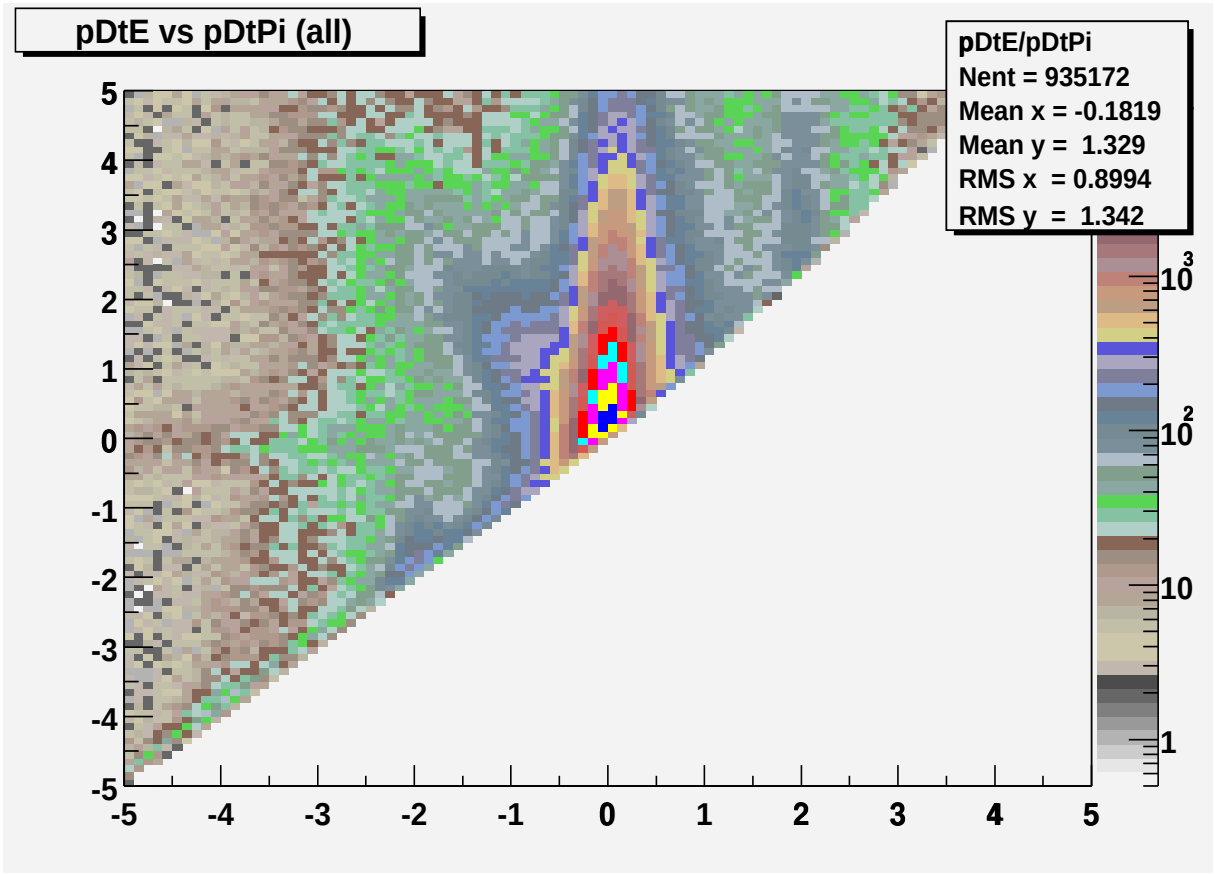

Figure 4: The same as in Fig. 1, but for the positive relativistic particle.

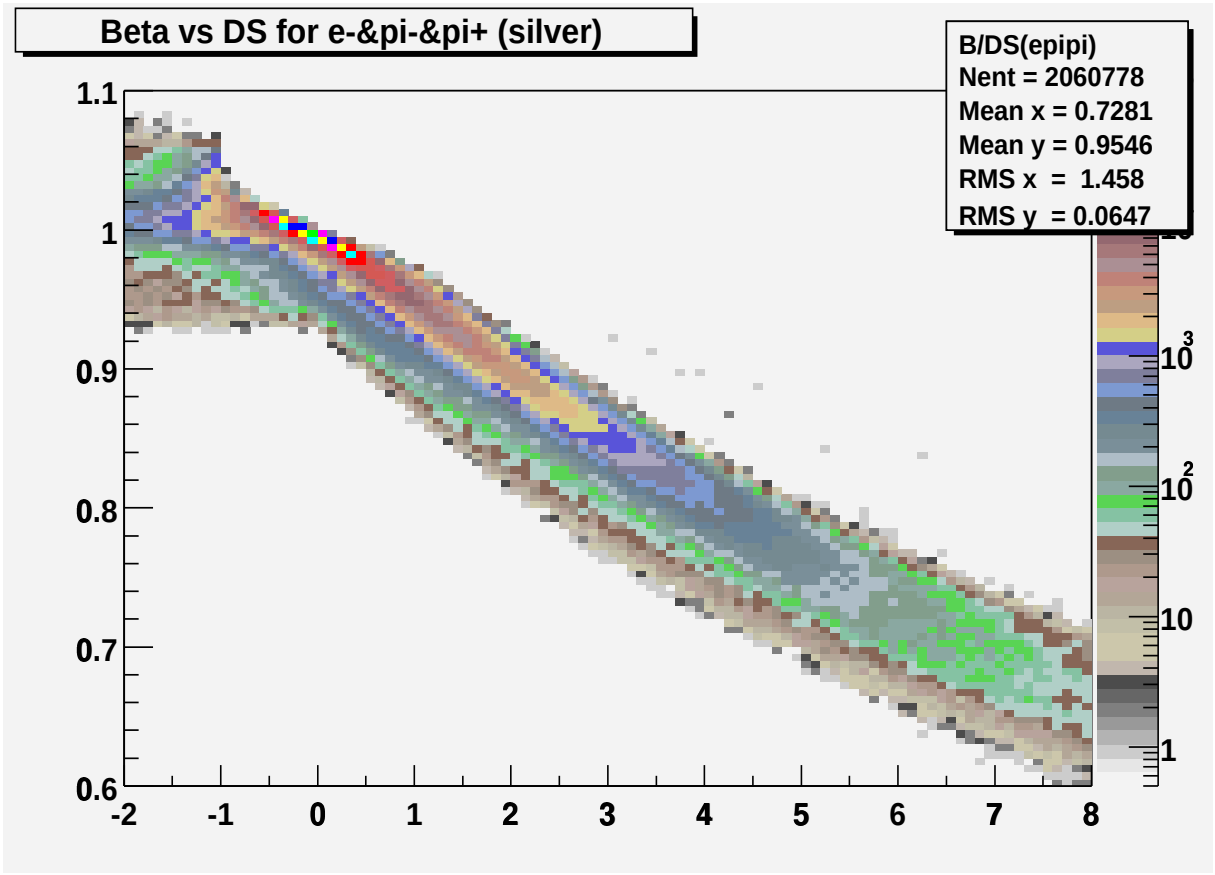

Figure 5: The dependence of the β for the all three relativistic particles as a function of the DS factor.

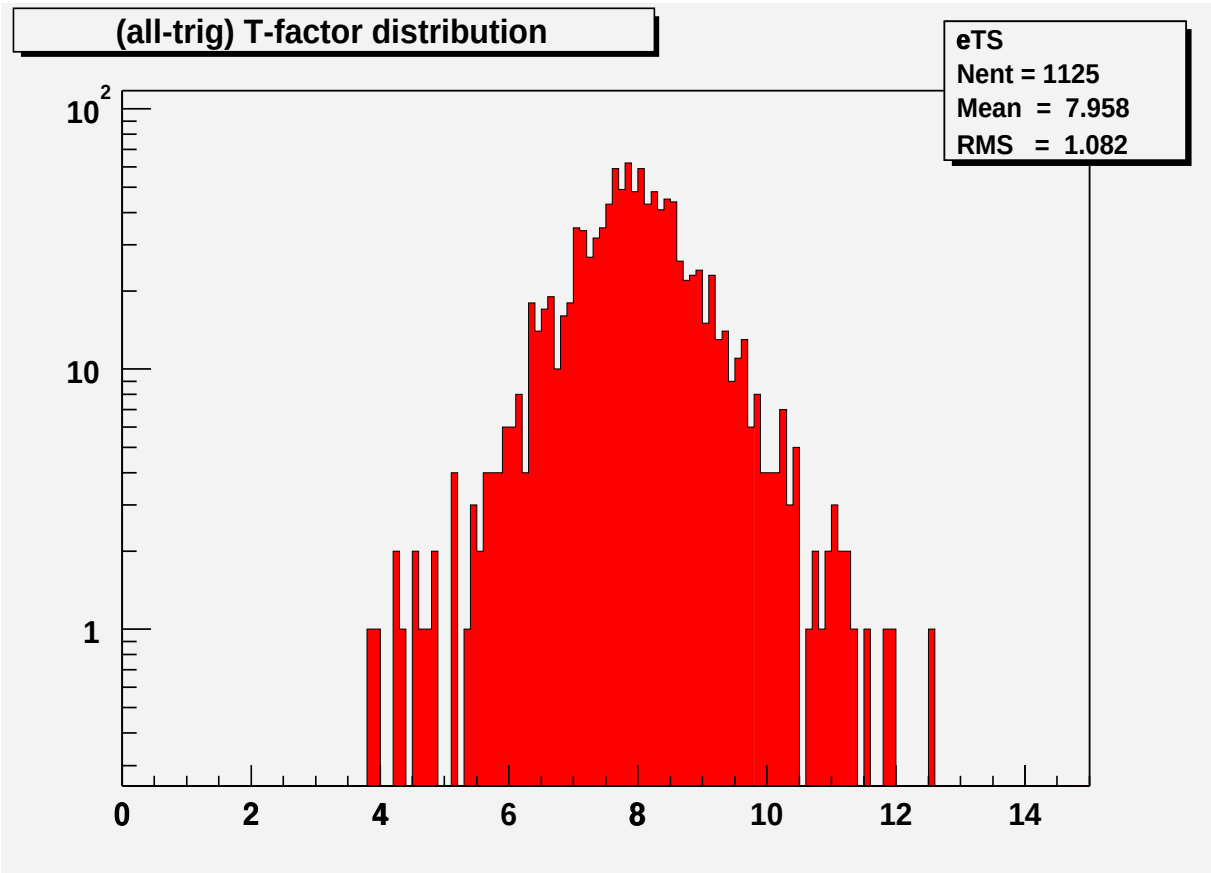

Figure 6: Distribution over the TS-factor for all three relativistic particles.

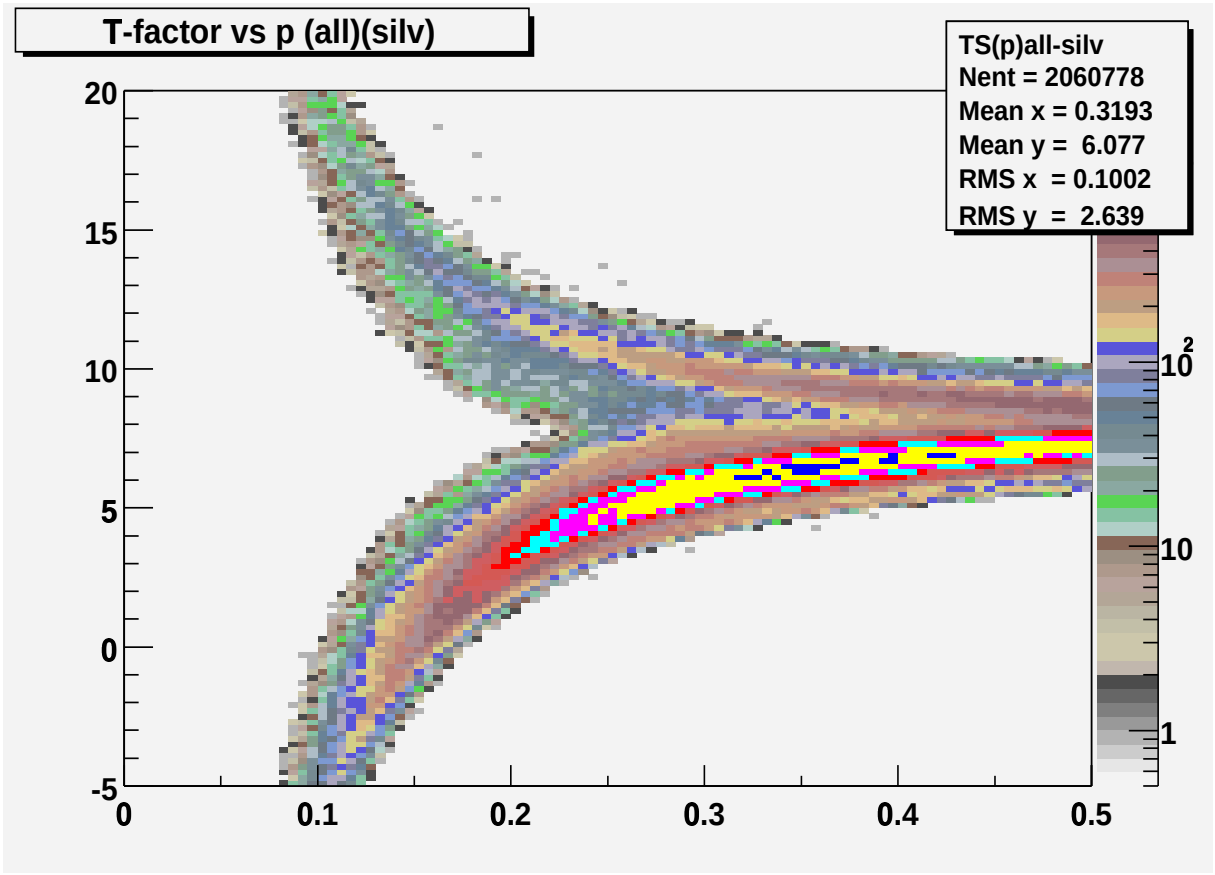

Figure 7: The TS-factor as a function of the momentum.

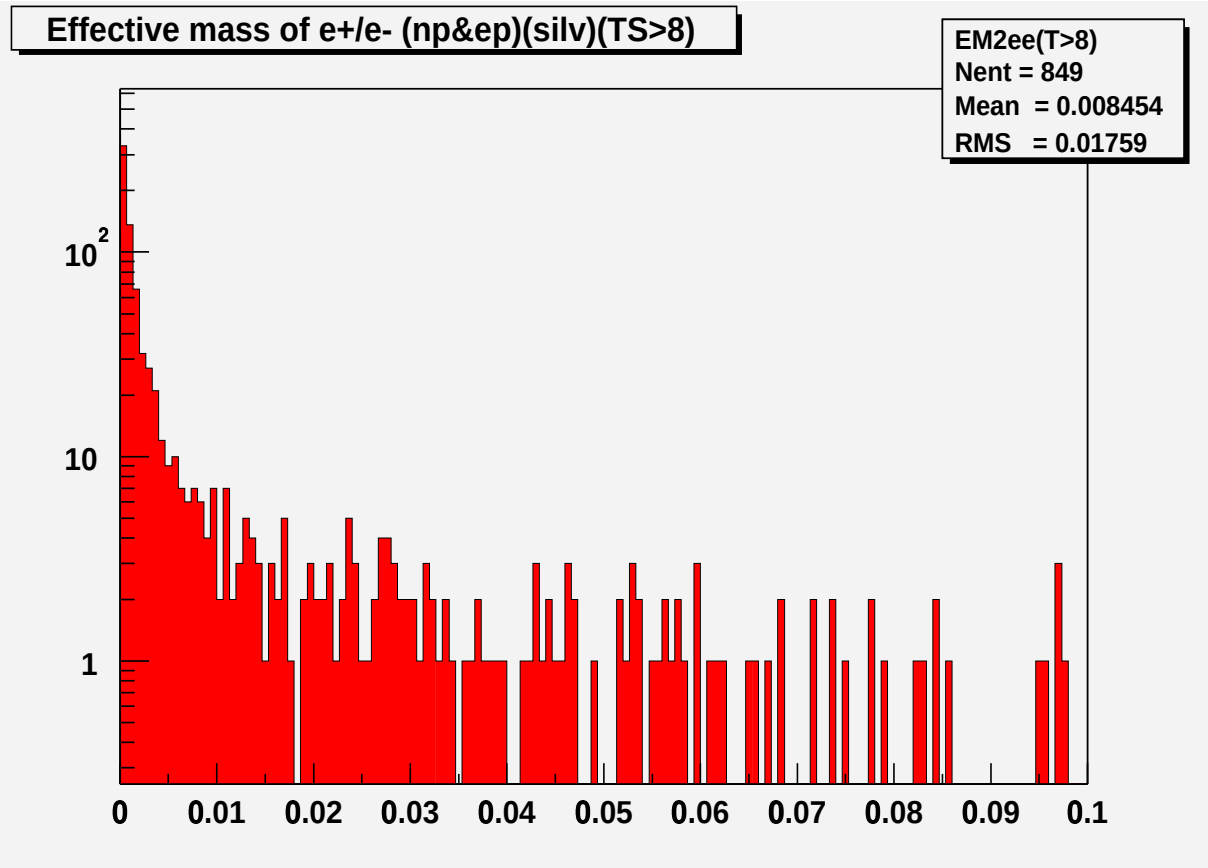

Figure 8: Distribution over the effective mass of the soft e^+e^- pairs for both e-pos and neg-pos combinations (see text).

electron or the positron radiated a gamma quanta after they have converted in the matter from the primary gamma. So these are the events of the electromagnetic shower development in CLAS before EC. This result opens a possibility to use the soft Dalitz pairs as an additional "detector" of photons in CLAS.

For comparison the distribution over the $\gamma\gamma$ effective mass is shown on the same scale in Fig. 10. Just to clarify why on the upcoming pictures the vector meson signal in the $\pi^+\pi^-$ system is small, it is necessary to point out that at this small energy and still relatively high Q^2 the production of η is small and on the histogram at 0.3 GeV^2 it is not seen at all (one should take into account, that two additional pions in the reaction match the η production threshold to the ω production threshold). On the other hand a clear maximum is seen for the zero effective masses. This is one more "ghost", which appears, when the second photon is disentangled as a ghost of the first real one. A good advise is to merge such "photons" in one.

4 EC, the Trigger cut, and the PS-factor of separation.

The EC signal as a function of momentum is shown separately for all three kinds of the relativistic particles in Fig. 11-13. The $E_{in} = ein_{ECPB}/.272$ and $E_{out} = eout_{ECPB}/.272$, $E = E_{in} + E_{out}$. In Fig.11 a clear maximum for electrons with E=p is seen. On the same picture only a small indication to pions (E=0.3 GeV) is visible.

On the contrary, in Fig.12 the signal of pions dominates. In addition there is a half-energy brunch of pions (or muons, which are not distinguished from pions in this paper), when only one of the E_{in} and E_{out} signals was disentangled. As the soft relativistic particles are not under consideration, the trigger condition E>0.2 GeV was used. With such a trigger the low brunch disappears.

Nevertheless it is interesting that this half-energy brunch is much less prominent for the positive relativistic particles (Fig. 13). As a result the events with E=0 (when both E_{in} and E_{out} have not been disentangled) are clearly visible. So the trigger cut (the "gold" cut) is formulated as: $E_{in} > .05$ GeV AND $E > 0.2$ GeV AND $N_{p.e.} > 0$ for all three relativistic particles ($N_{p.e.} = nphe_{CCPB}$). For generality the LAC was considered in the sample, but after the trigger cut the LAC contribution becomes negligible, as the CC does not cover it.

The resulting E(p) distribution for the second negative relativistic particle after the trigger cut is shown in Fig. 14. The trigger suppression is so effective that the pions becomes clearly visible on the plot in comparison to the Fig. 12. The "gold" cut includes the "silver" cut (timing cut, described above).

As a result of the analysis of the E(p) plots the P-selector (PS-factor) was defined as $PS = \frac{E-.2}{|p-.2|}$. The distribution over the PS-factor of the events with the trigger cut for all three kinds of the relativistic particles is shown in Fig.15 . The pions are expected near zero and the electrons near unit. The intermediate area is filled by the low energy relativistic particles, where the TS-factor is expected to be effective. That is why a combination of the two factors must make better separation.

The PS(TS) plot for all three kinds of the relativistic particles with the "gold" cut are shown in Fig. 16. The resulting PT-selector (PTS-factor) was defined as $PTS = TS + 4 \cdot PS$. The distribution over the PTS factor is shown in Fig. 17.

5 CC and the CS-factor of separation.

The Cerenkov counter looks like an independent detector as it just gives a number of photo electrons as a response to the particle crossing. But in fact it is not as it is multi-sectional detector subdivided in θ.After the DC track of the charged particle matches the cluster in EC, it becomes possible to distribute the signals from CC over θ in respect to the θ_0, which is defined by the straight line from the reaction vertex to the EC cluster. The bigger deflection of the θ from the θ_0, the bigger the quality factor ($QC = chi2cc_{CCPB}$). The $N_{p.e.}$(QC) distribution is shown in Fig. 18. The two branches are obvious: one has a big number of photo

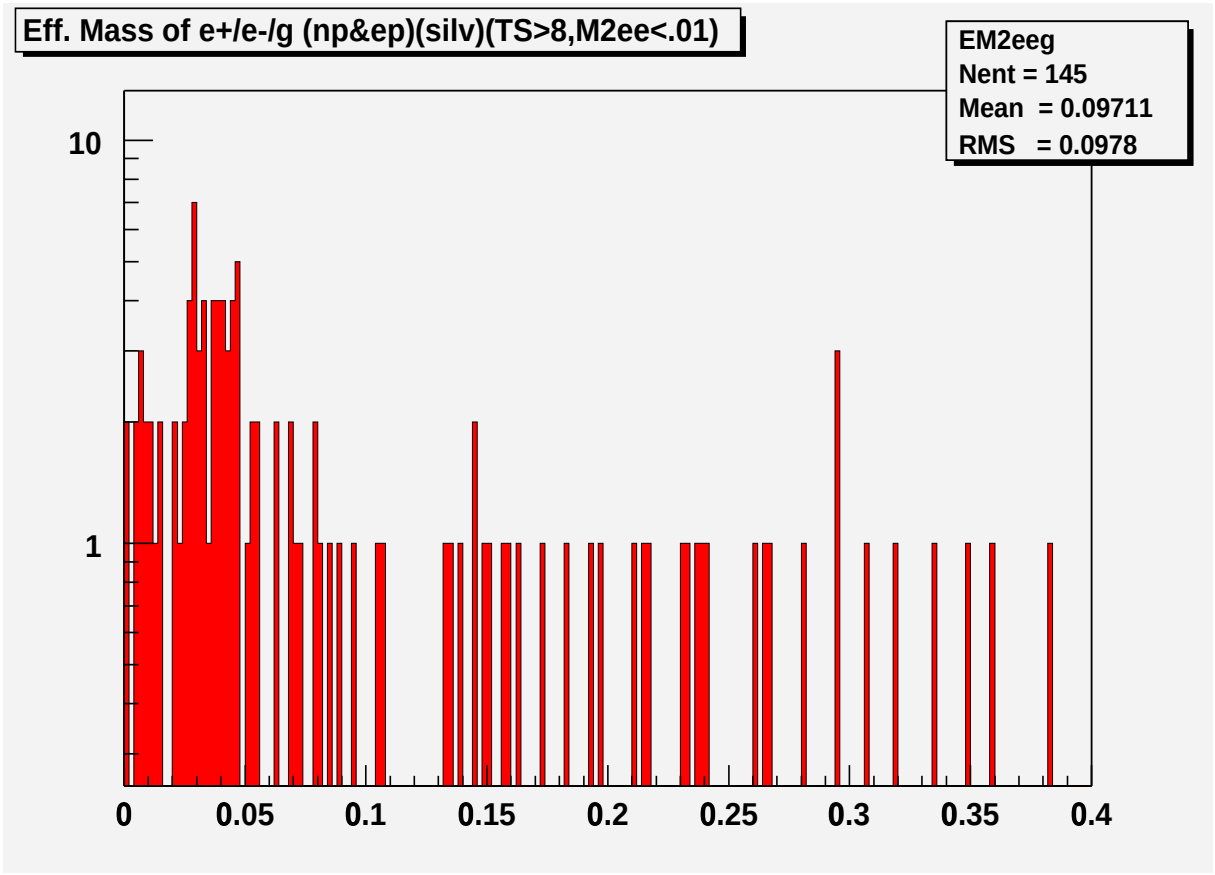

Figure 9: Distribution over the $e^+e^-\gamma$ effectiv mass when both e^+ and e^- are soft.

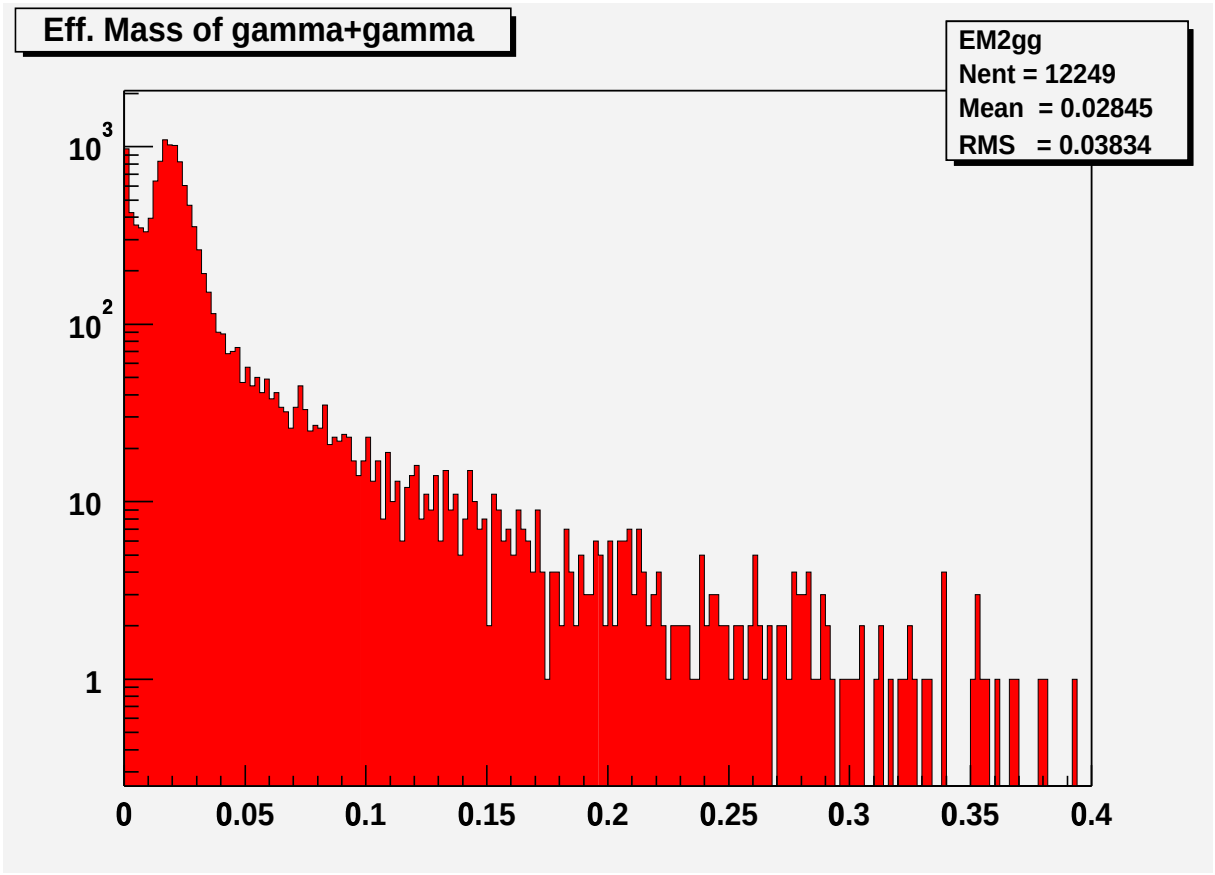

Figure 10: Distribution over the $\gamma\gamma$ effective mass.

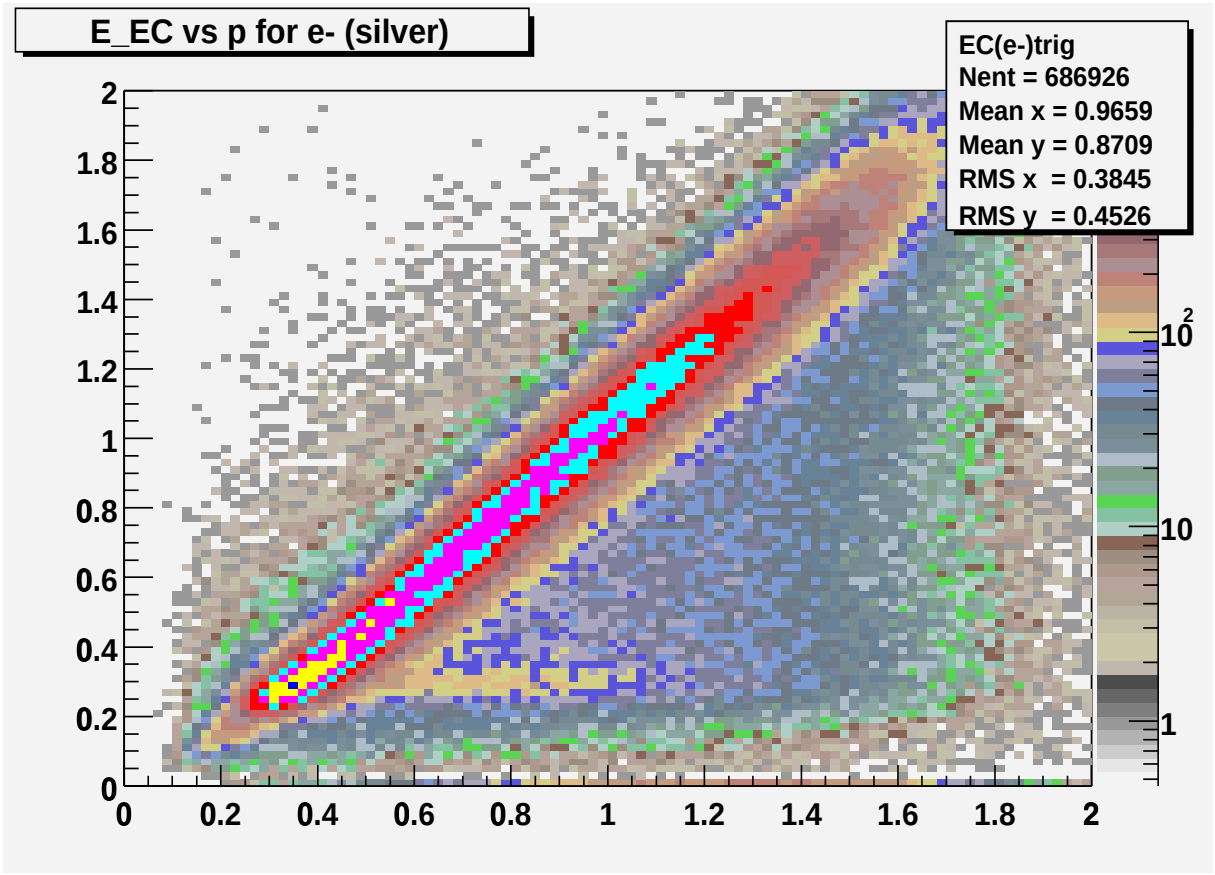

Figure 11: EC energy as a function of momentum for scattered electrons.

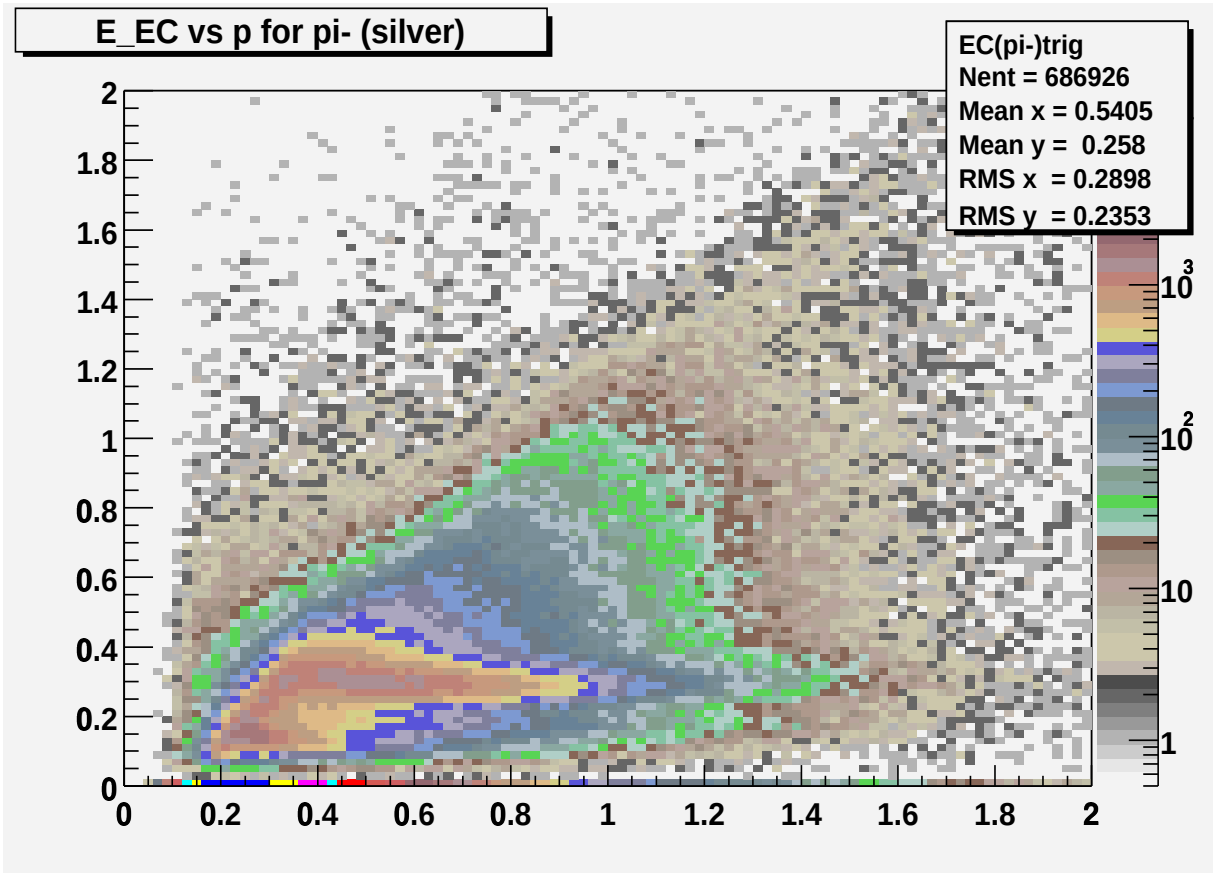

Figure 12: EC energy as a function of momentum of the second negative relativistic particle

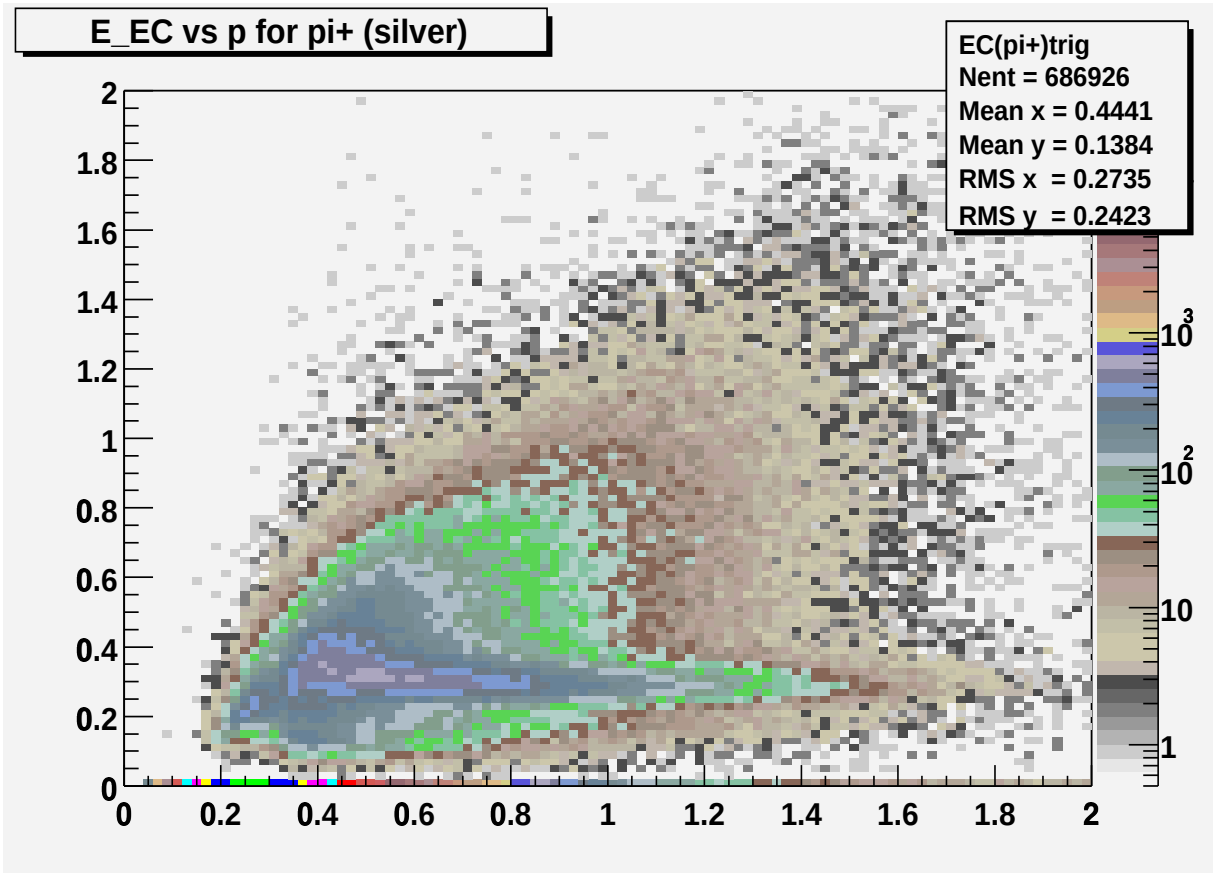

Figure 13: EC energy as a function of momentum for the positive relativistic particles.

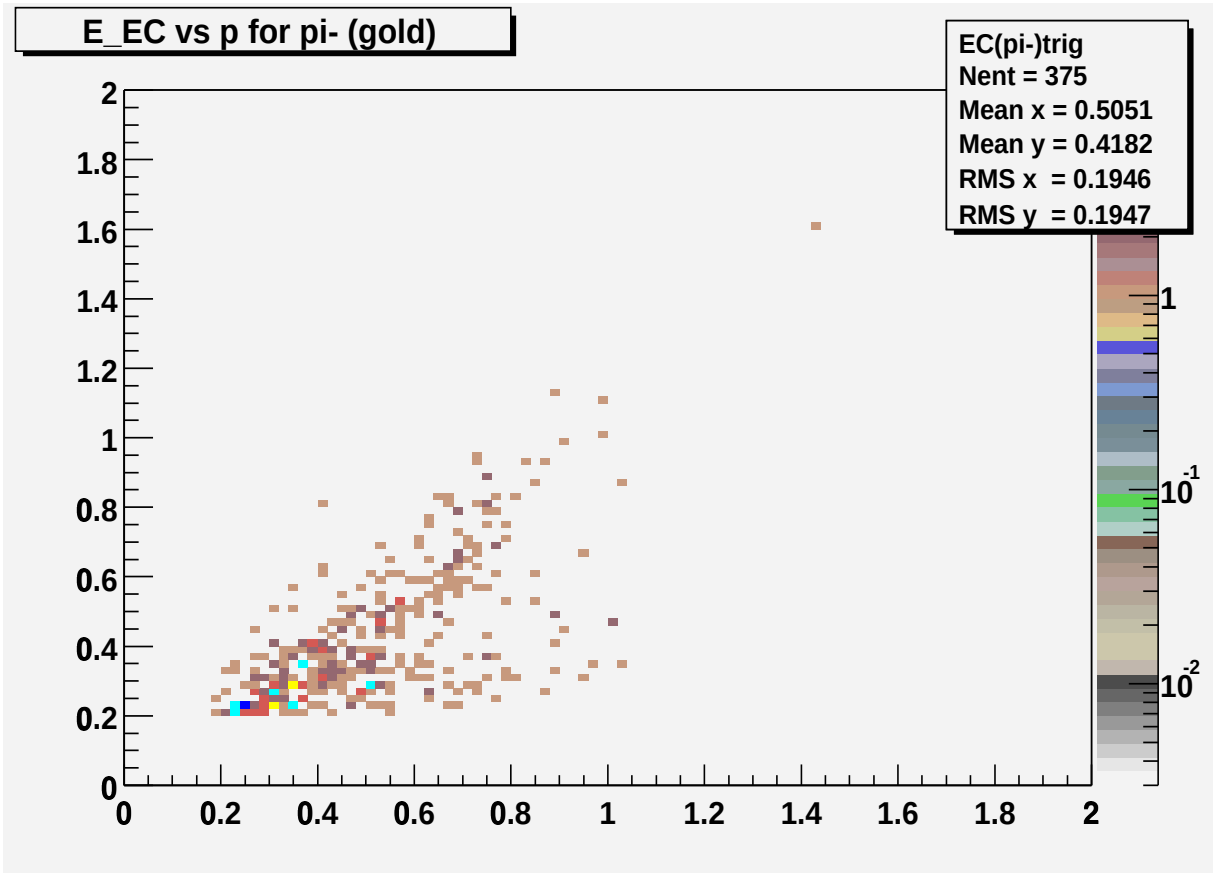

Figure 14: EC energy as a function of momentum for the scattered electrons after the trigger cut (see text)

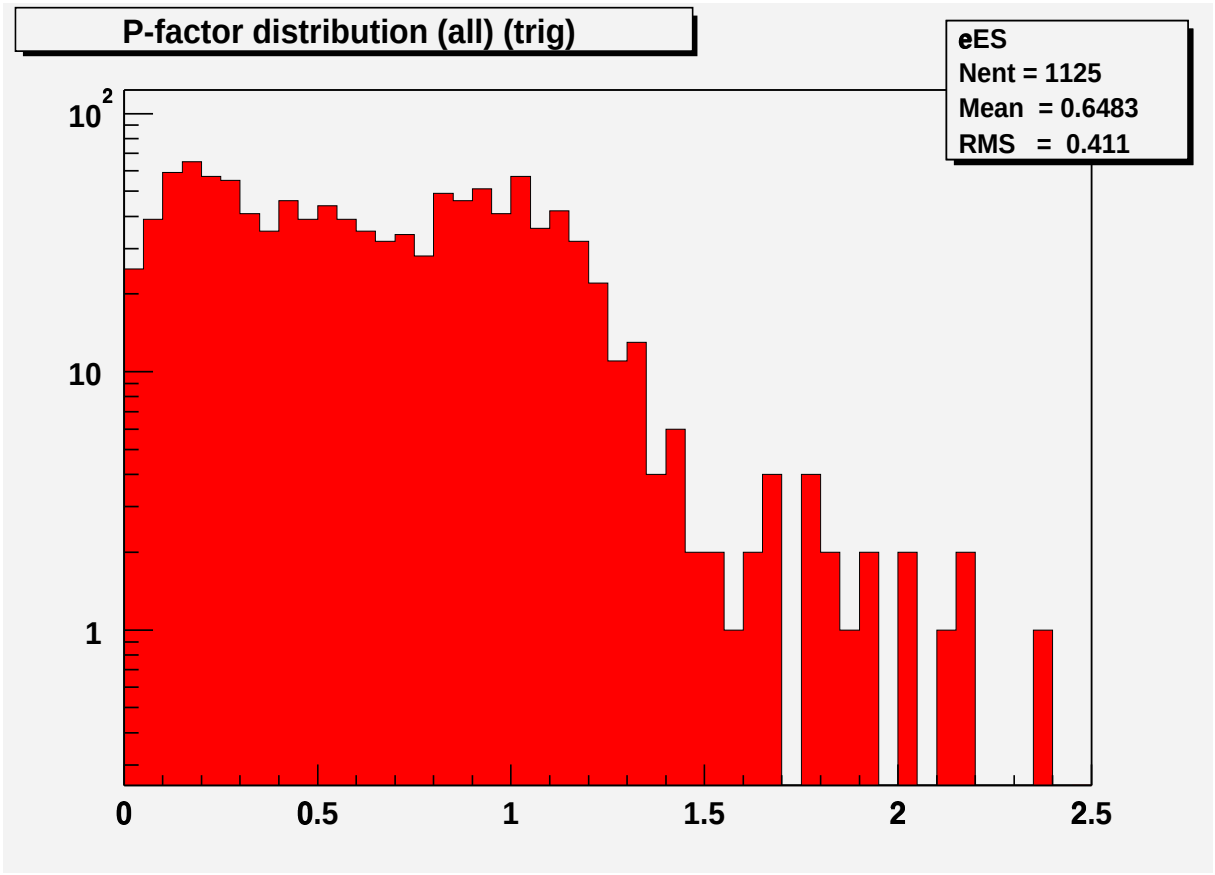

Figure 15: PS distribution (with the trigger cut) for all three kinds of the relativistic particles.

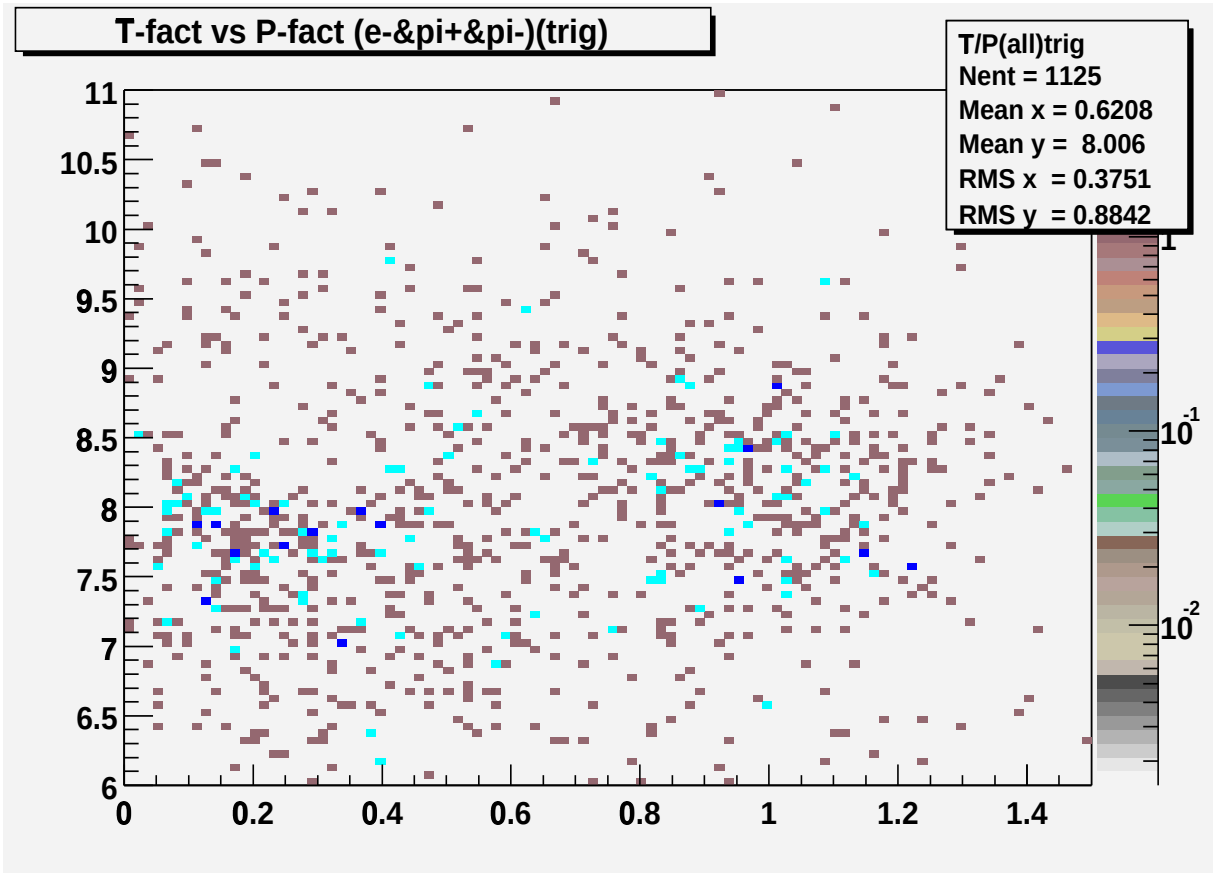

Figure 16: The PS(TS) plot for all relativistic particles with the "gold" cut.

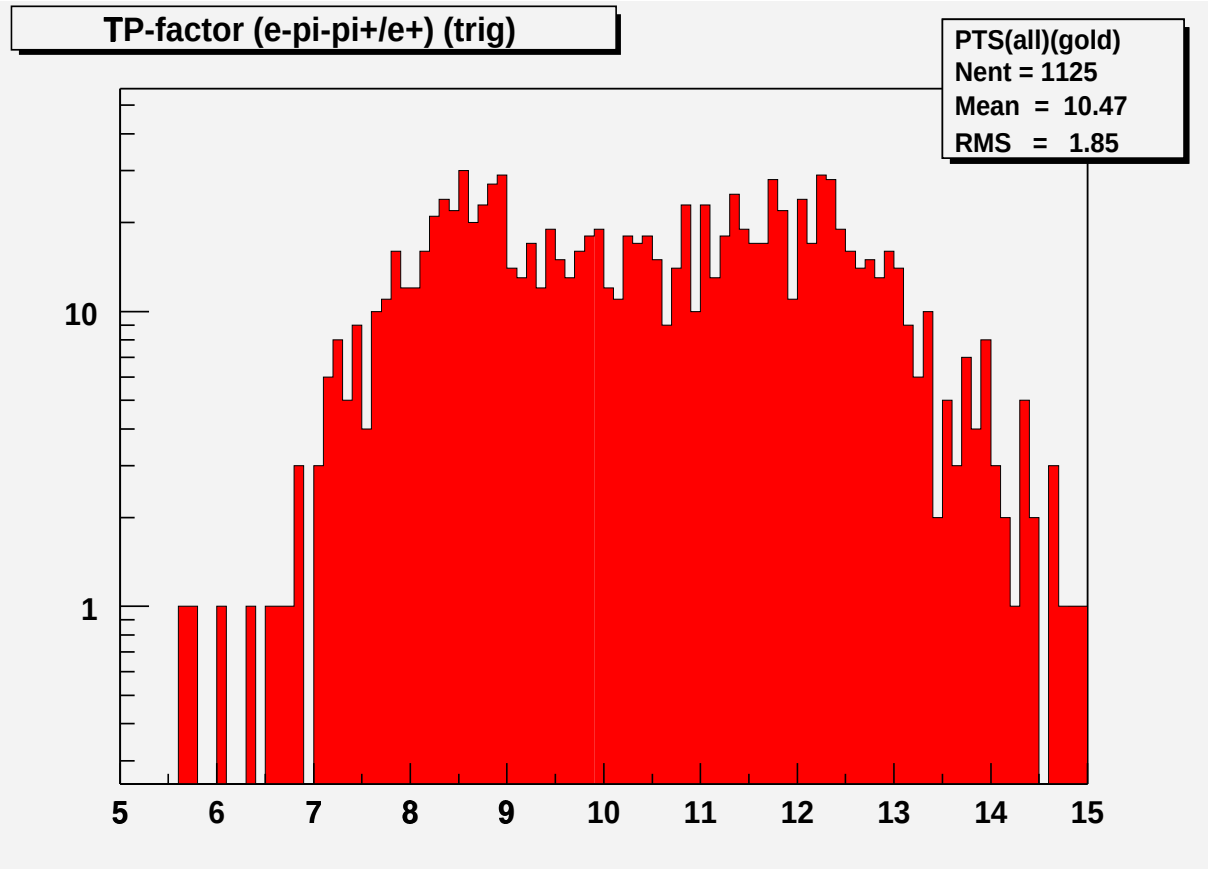

Figure 17: The distribution of the all relativistic particles over PTS-factor with the "gold" cut.

electrons (in fact the value in the CCPB bank is 10 times bigger than the real number of photo electrons) and a good (small) quality factor - these are electrons, and the other has a small number of photo electrons and a bad (big) quality factor - these are pions. In the region of the small number of photo electrons and a small quality factor the pions and electrons are indistinguishable for the Cerenkov counter.

The same distribution but for the "gold" events is shown in Fig. 19. The picture keeps the same.

Unfortunately for the positive relativistic particles the quality factor in CC is still must be improved. The similar distribution for the positive relativistic particle is shown in Fig. 20. If the quality factor for the positive particles is improved it can help to improve the separation procedure significantly.

The C-separator (CS-factor is defined as CS=$\frac{400 \cdot QC - N_{p.e.}}{400 \cdot QC + N_{p.e.}}$. It is close to 0 for electrons and to 1 for pions. The PTS(CS) plot is shown in Fig. 21. On the basis of this plot the CPT-separator (CPTS-factor) was calculated as $CPTS = PTS - 4 \cdot CS = TS + 4 \cdot PS - 4 \cdot CS$.

The distribution over the CPTS-factor is shown in Fig. 22. To be sure that these are real events of the $e^- r^+ r^- p$ topology, where r stands for the both relativistic particles e and π, and to define the $\frac{e^-\pi^+\pi^- p}{e^- e^+ e^- p}$ suppression factor, the kinematic cut for this kind of reactions is necessary.

To reduce the background of other reaction it is necessary to make a kinematic analysis of all four final particles, including the proton. To disentangle the reaction, the two kinematic values were calculated: the missing mass for the $(e^-, e^-\pi^+\pi^-)$ reaction ($mm^2_{e^-\pi^+\pi^-}$) and the energy and momentum conservation factor $\Delta^2 = (E^e_{in} + M_p - E^{\pi+}_{out} - E^{\pi-}_{out})^2 + (\vec{p}^{\,e}_{in} - \vec{p}^{\,e}_{out} - \vec{p}^{\,\pi+}_{out} - \vec{p}^{\,\pi-}_{out})^2$. The $\Delta^2(mm^2_{e^-\pi^+\pi^-})$ plot is shown in Fig. 23. In addition to the parabolic smearing in case of the error in the momentum measurements, there is additional contribution of the $e^- r^+ r^- \pi^0 p$ reaction above the $mm^2_{e^-\pi^+\pi^-}$>1.16 GeV^2 limit,. There should be the photon radiation smearing to the right of the $mm^2_{e^-\pi^+\pi^-}>M_p^2$ line too. Both processes do not change the topology of the charged particles in the reaction, and the cut is mostly used to suppress the random combinations at high multiplicity.

Another problem is associated with the identification of positive particles in the reaction. The percentage of the misidentified positive particles can be estimated from the plot in Fig. 24, where the energy deposition in SC of the "proton" (dedx$_{SCPB}$) is plotted versus the energy deposition in SC of the "π^+", identified in CLAS in the cooking level. The clear horizontal maximum, corresponding to the misidentified positive particle is seen, but the π/p separation can be an issue of another task.

The kinematic cut was defined as 0.78<$mm^2_{e^-\pi^+\pi^-}$<1. GeV^2 AND Δ^2<.02 GeV^2. The kinematic cut with the "gold" cut makes the "platinum" sample. With this clean up cuts the π/e rejection looks much better (Fig. 25).

6 Separation of the $e\pi\pi p$ and $eeep$ reactions.

The developed separation factor was applied to both "e" and "neg" relativistic particles.The plot is shown in Fig. 26. The two imaginary lines eCPTS=10 and nCPTS=10 subdivide the plane in four parts. The eπ and πe events fill the top-left and the bottom-right parts correspondingly. The ee events fill the top-right part, but from the bottom left part it is clear that the electrons can be found up to the 8 boundary, so an inefficiency of ee pair detection of about 12% can be expected.

In Fig. 27 the nCPTS>10 AND eCPTS>10 cut is applied to the distribution of the positive relativistic particles. Finally with all previous cuts the number of the residual positive pions and positrons is equal. Now the last pCPTS>10 cut selects eee events. Only 10 out of the $2 \cdot 10^5$ "platinum" events are identified as the eee events.

The $\pi^+\pi^-$ effective mass distribution for all "platinum" events without the trigger cut is shown in Fig. 28. Only small maximum is seen at the position of the ρ meson. The explanation is the same as for the η above.

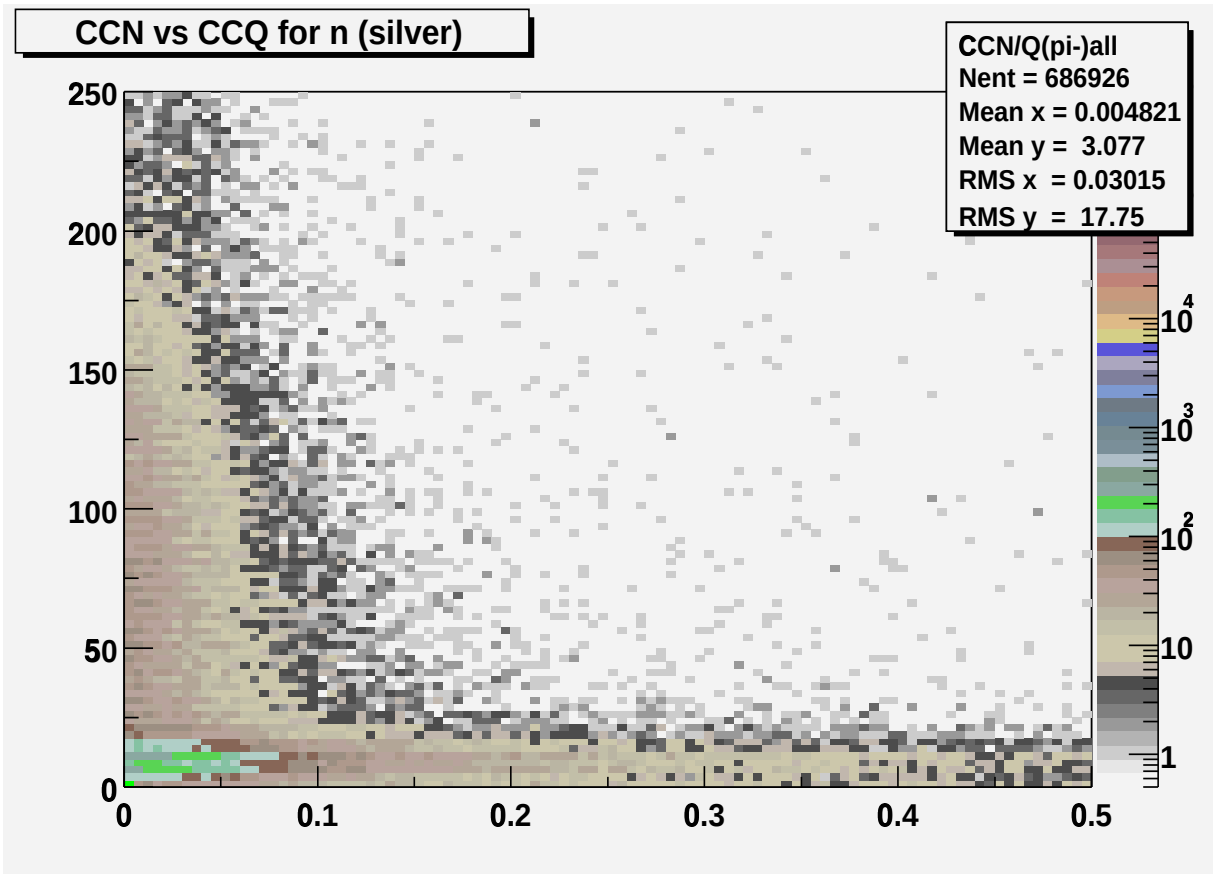

Figure 18: $N_{p.e.}$(QC) plot for the second negative relativistic particle ("silver" events).

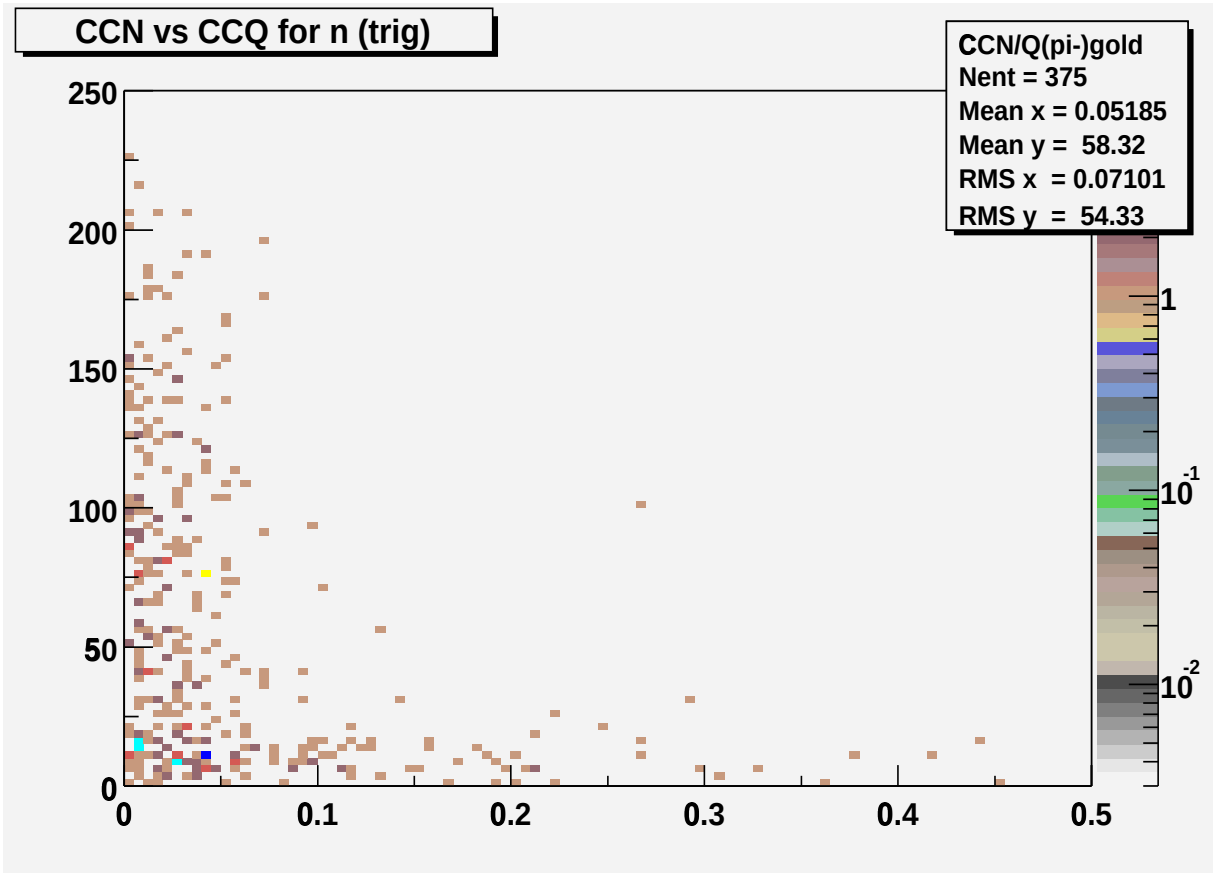

Figure 19: The same as in Fig. 18, but for the "gold" events.

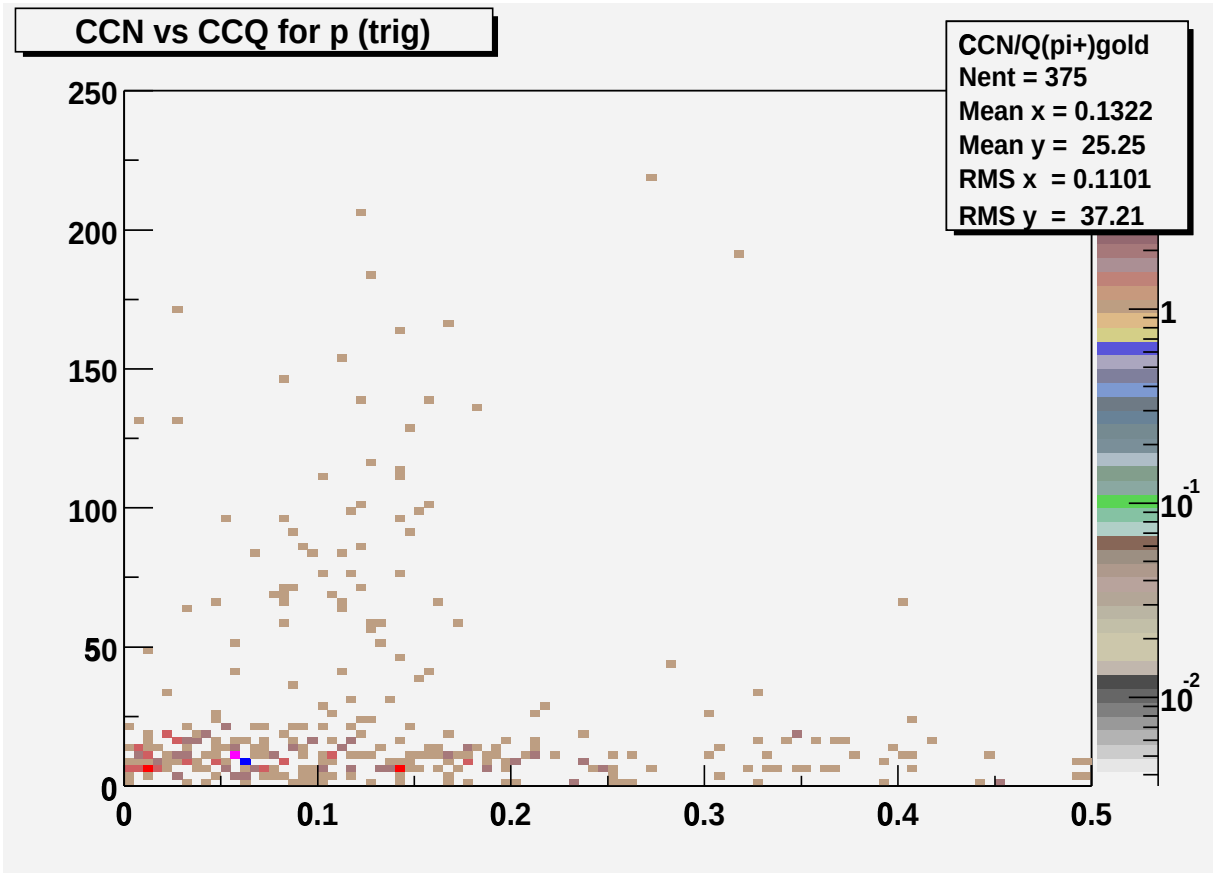

Figure 20: The same as in Fig. 19, but for the positive relativistic particle.

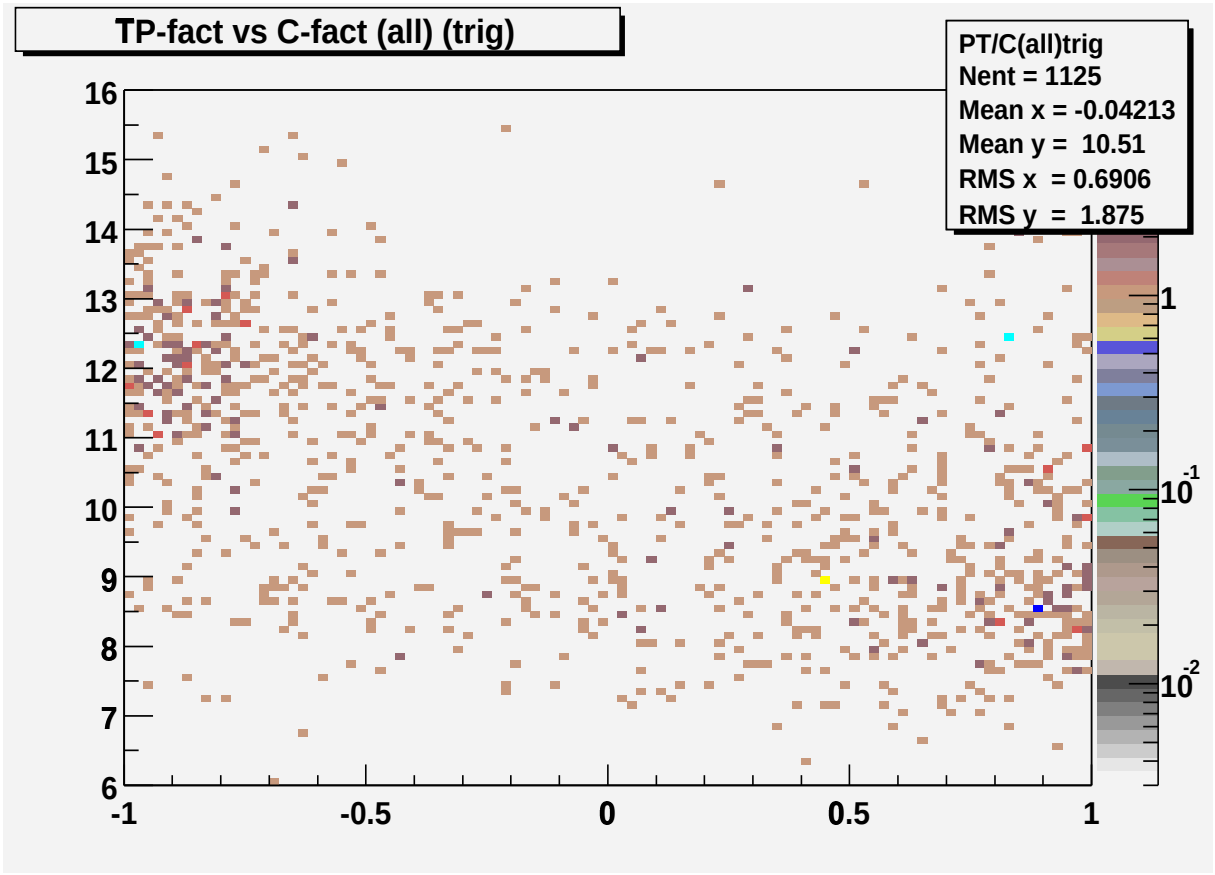

Figure 21: TPS vs CS plot for the "gold" events (all three relativistic particles)

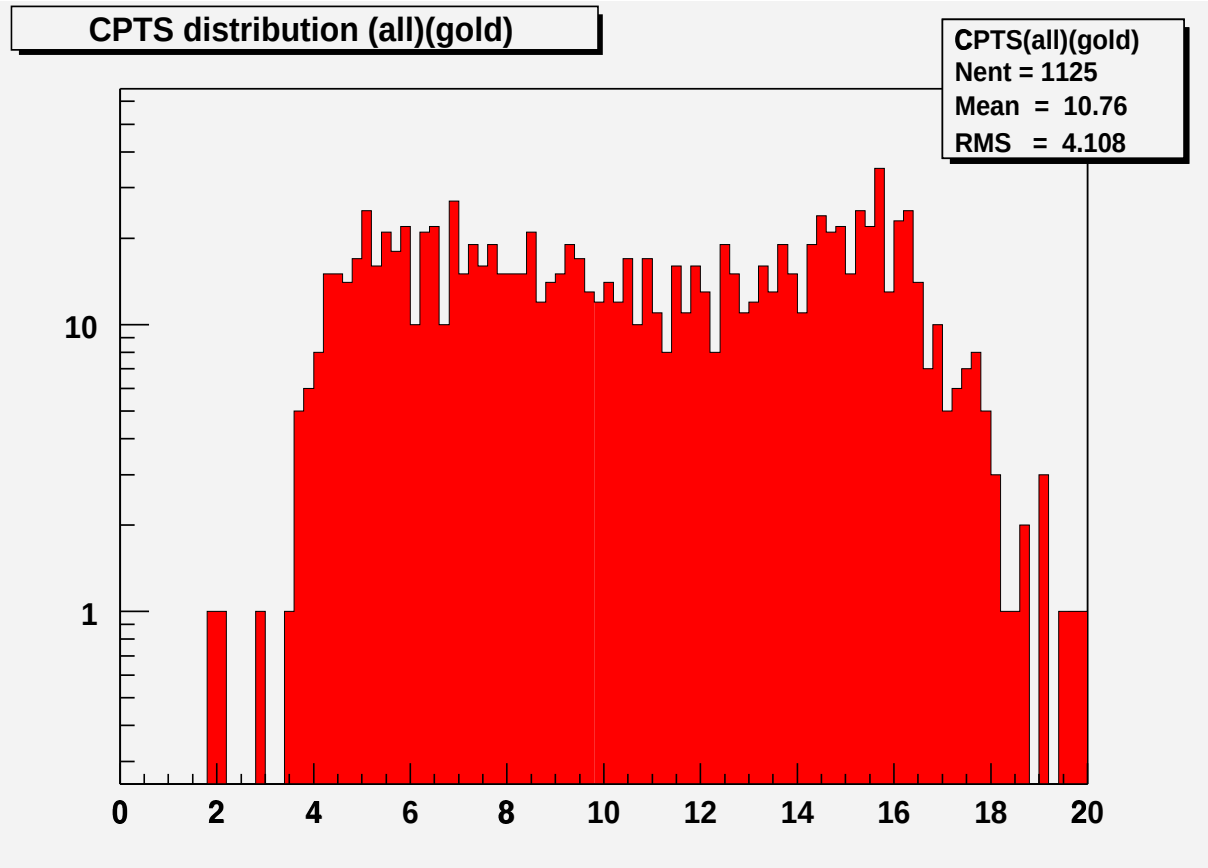

Figure 22: Distribution of the "gold" events over the combined separation factor CPTS (all three relativistic particles).

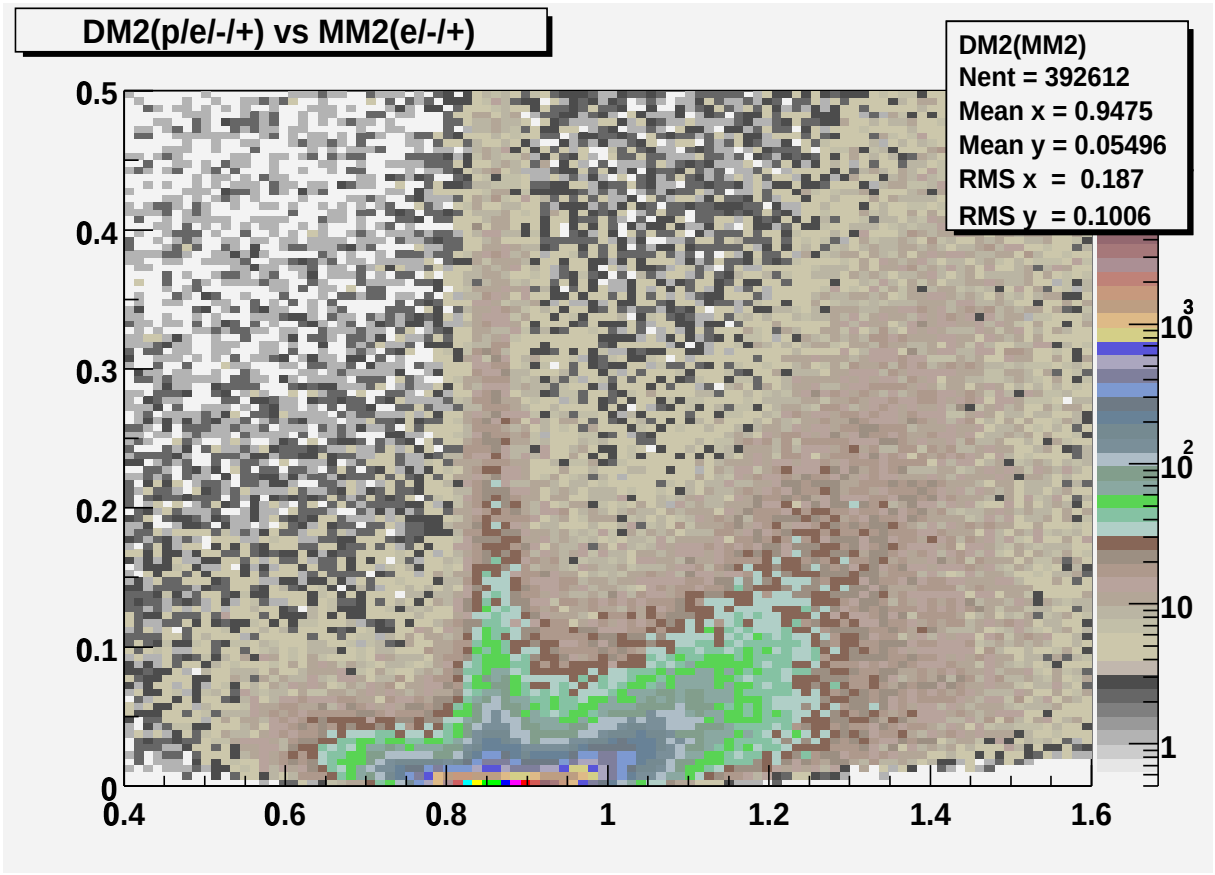

Figure 23: Energy-momentum conservation factor versus the missing mass for the three relativistic particles.

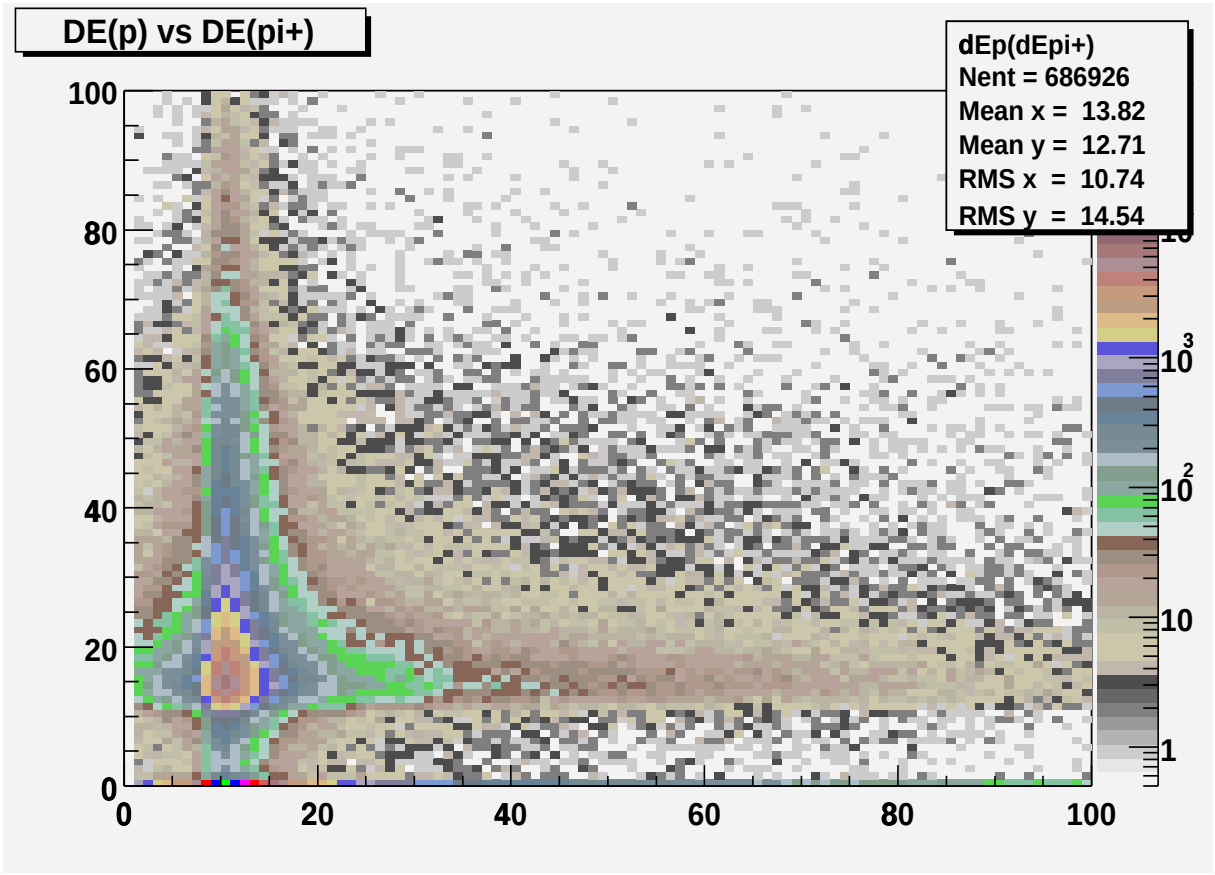

Figure 24: Energy deposition of the "proton" versus the energy deposition of the "π^+".

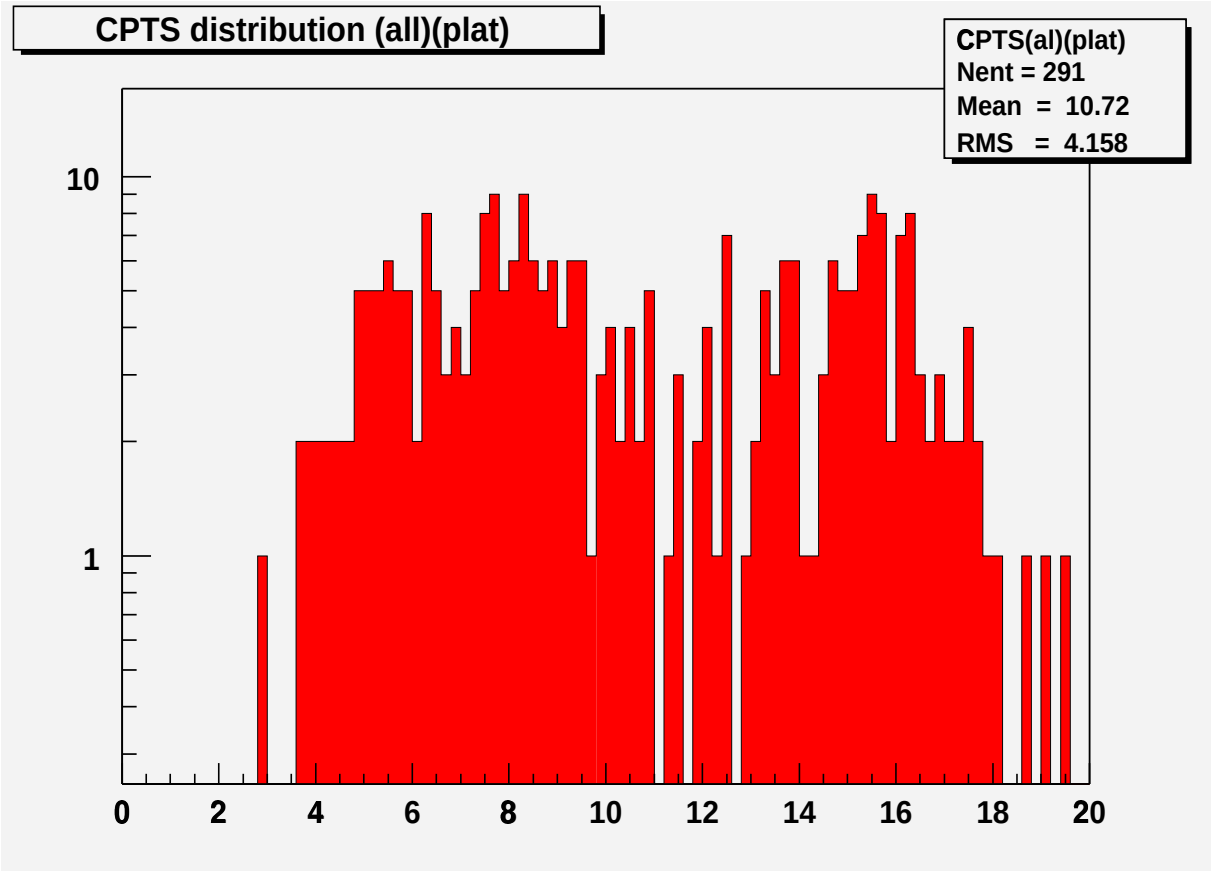

Figure 25: The same as in Fig.22, but for the "platinum" events.

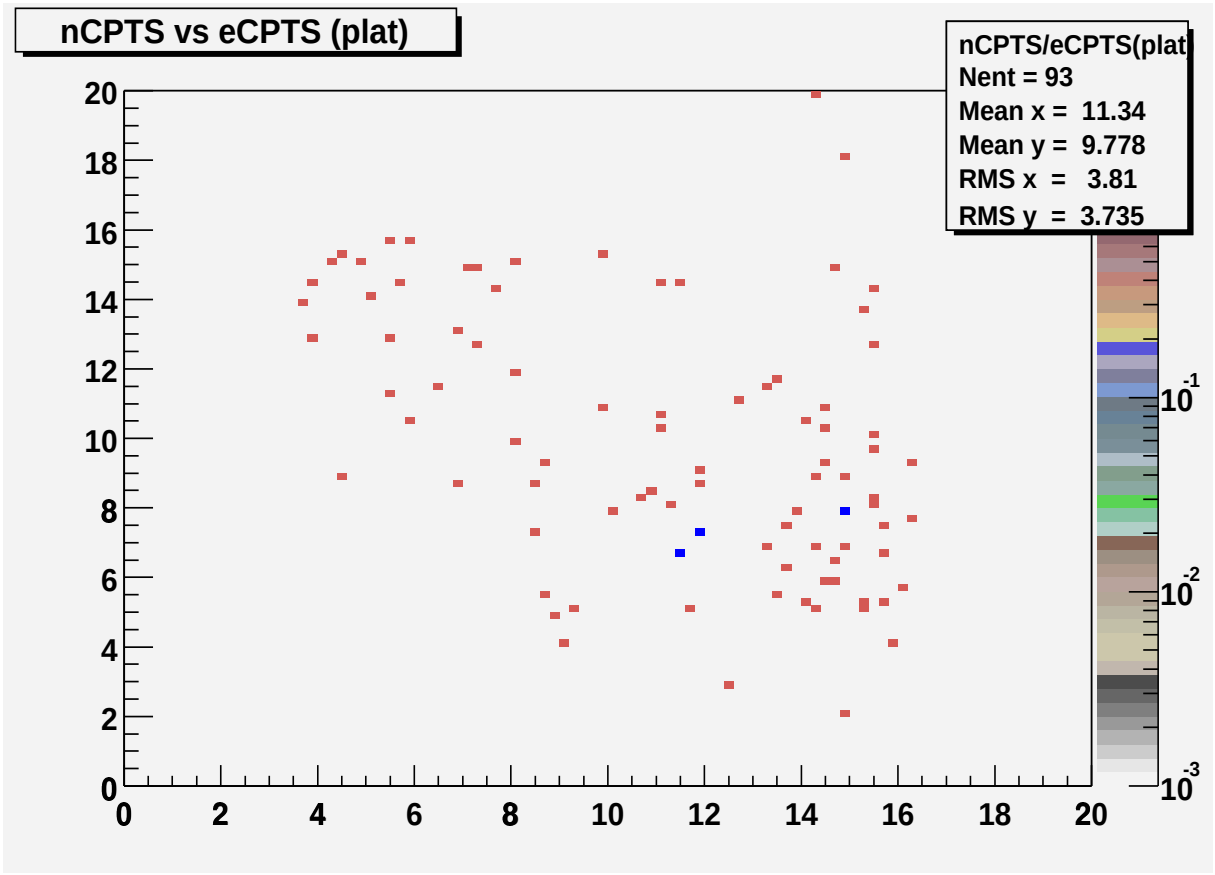

Figure 26: Separation of negative particles.

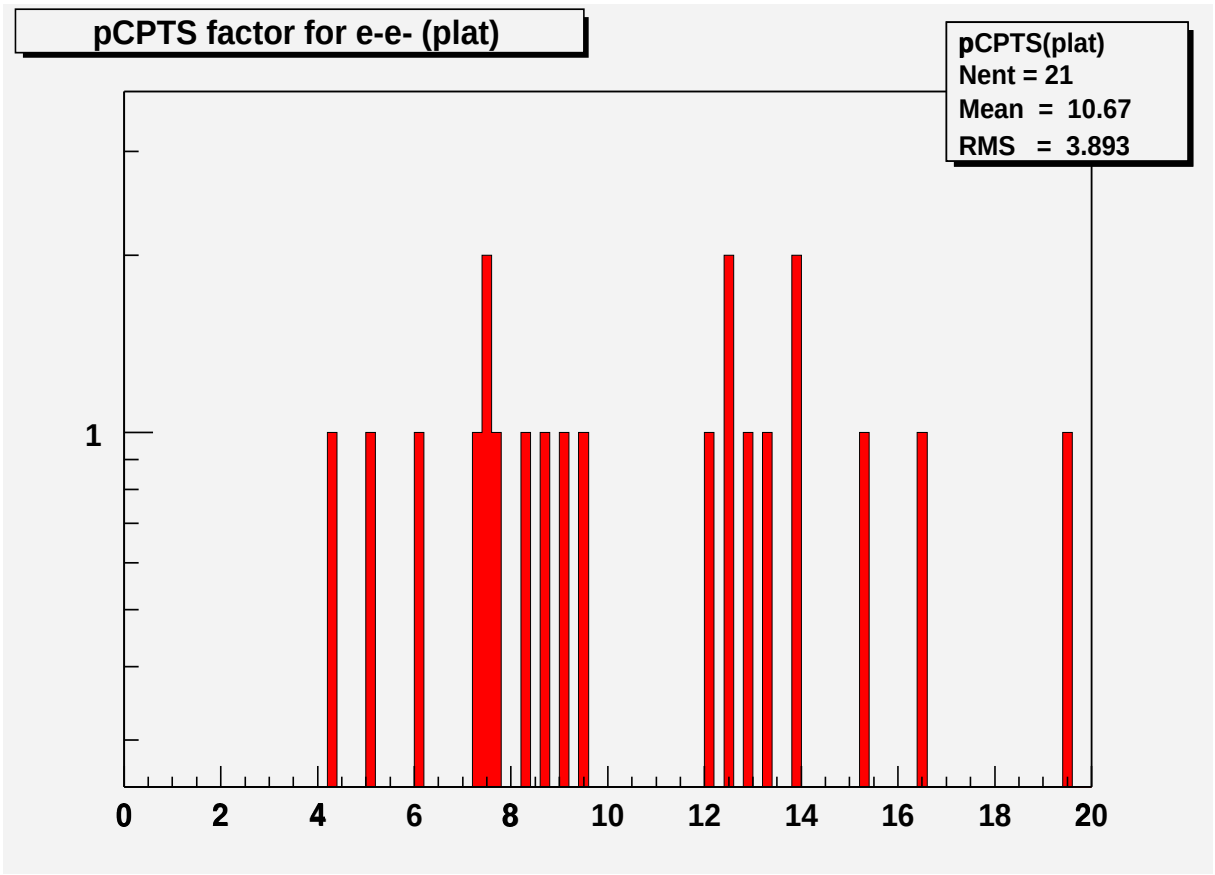

Figure 27: Separation of the positive relativistic particles after the e^-e^- sample is selected ("platinum" events)

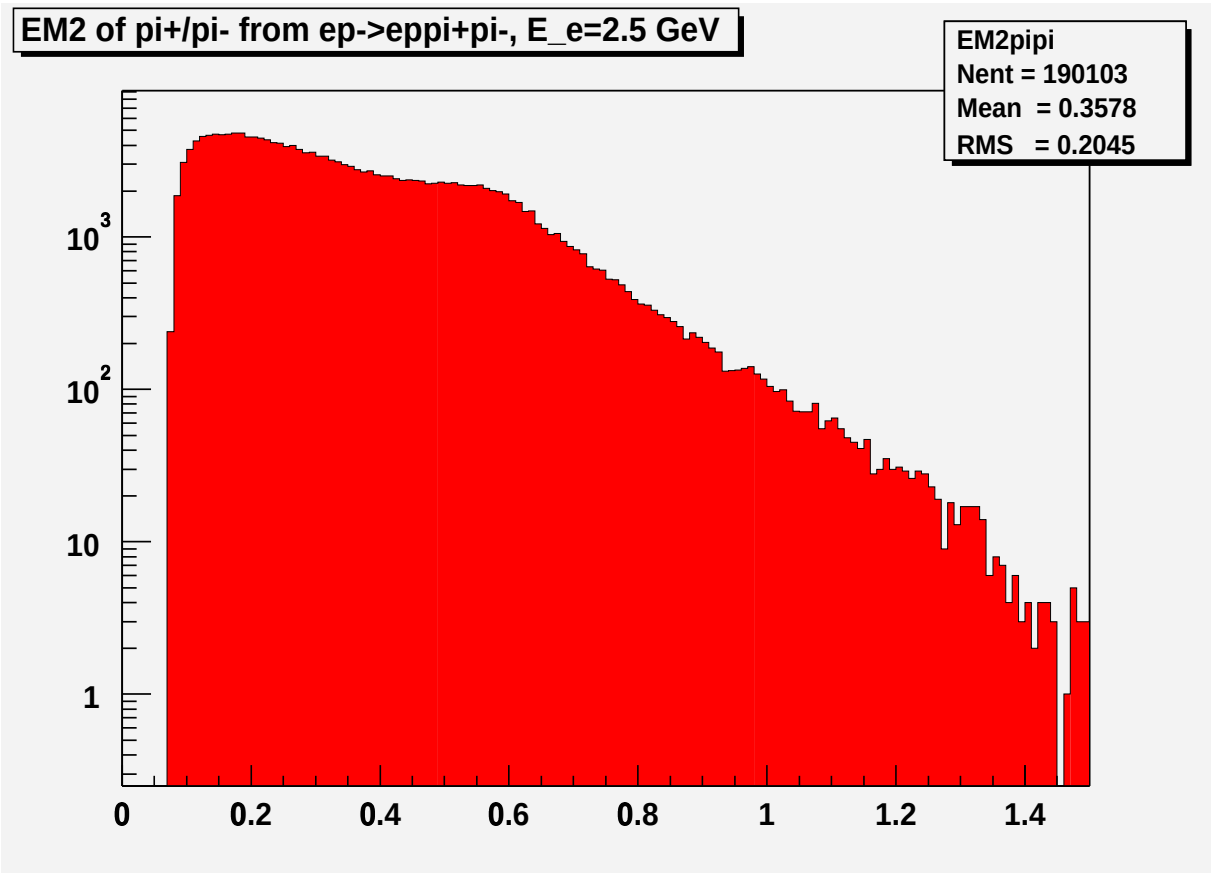

Figure 28: Effective mass of two pions for the "platinum" events without the trigger cut.

The distribution over the effective mass for the selected *eee* events is presented as a two-dimensional plot as the two e^+e^- combinations exist for each *eee* event. The plot is shown in Fig. 29. So only one event is a candidate to a real vector meson decayed in e^+e^- and the rest pairs are Dalitz conversions (two of them are too close to each other at (0,0.66)). It means that the rejection of the $\pi\pi$ decays is better than $5{\cdot}10^{-6}$.

To see the effective mass distribution for the Dalitz pairs in better scale, the histogram of the minimum value of two above was made (Fig. 30).

The same histogram was made for all "platinum" events (Fig. 31). so only 2 out of 11 Dalitz pairs are missing. So the ee-efficiency can be estimated as 82±18%. This estimate is consistent with the estimate from the plot in Fig. 26, which is 88±4%.

7 Conclusion.

In spite of the fact that the electron runs at low energy (which is necessary to make a test at proper energy of the secondary relativistic particles) produce only a small amount of the vector mesons (in comparison to the equivalent photon runs), the test of the $\pi\pi$ suppression on the sample of the e1c run is successful because the $\Delta^0\pi^+$ and $\Delta^{++}\pi^-$ final states are even better as they do not produce e^+e^- pairs. The $5 \cdot 10^{-6}$ value for the $ee/\pi\pi$ ratio, which was found in the paper, is approximately the number which is expected for the real e^+e^- pairs from the ρp final state. It means that the CLAS detector is ready to measure the distribution over the effective mass of the vector mesons using the e^+e^- decay channel.

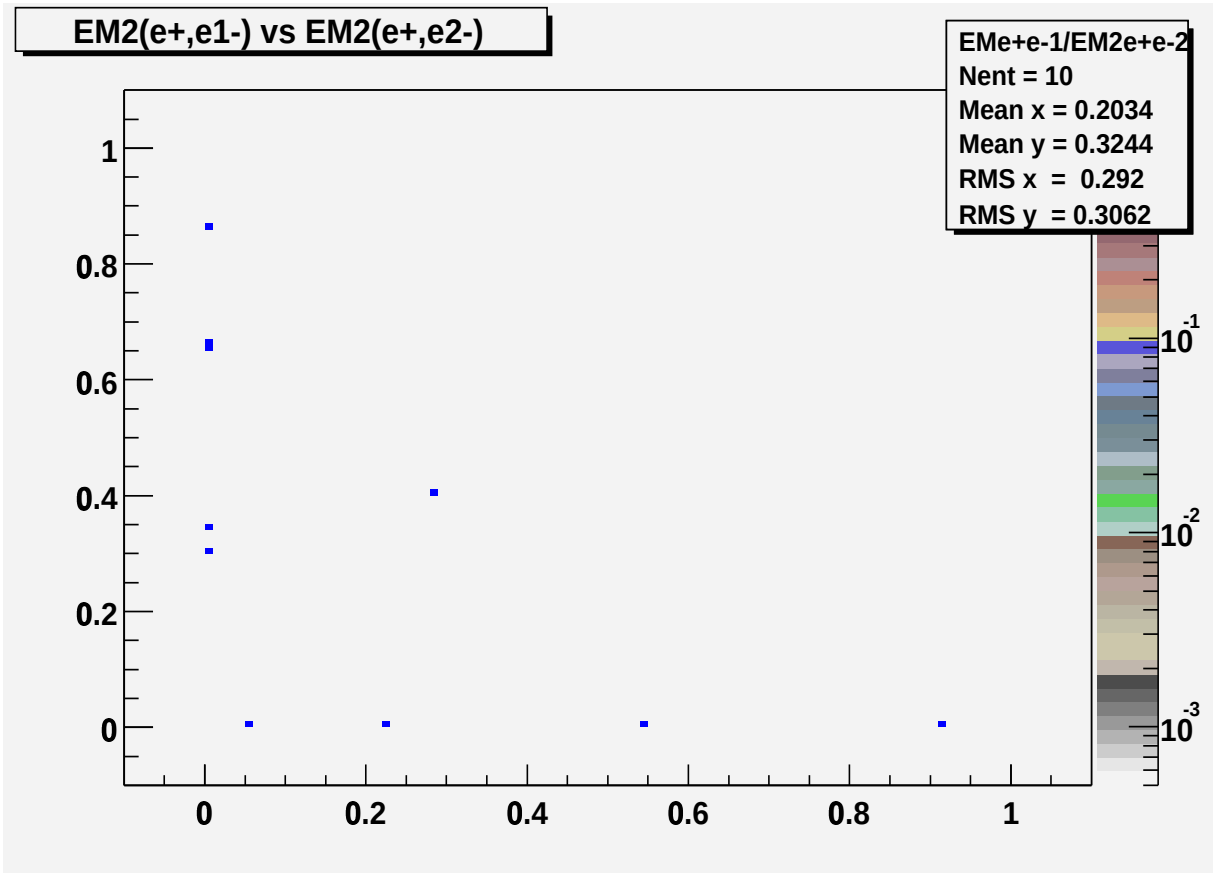

Figure 29: Effective mass distribution of the eee events (see text)

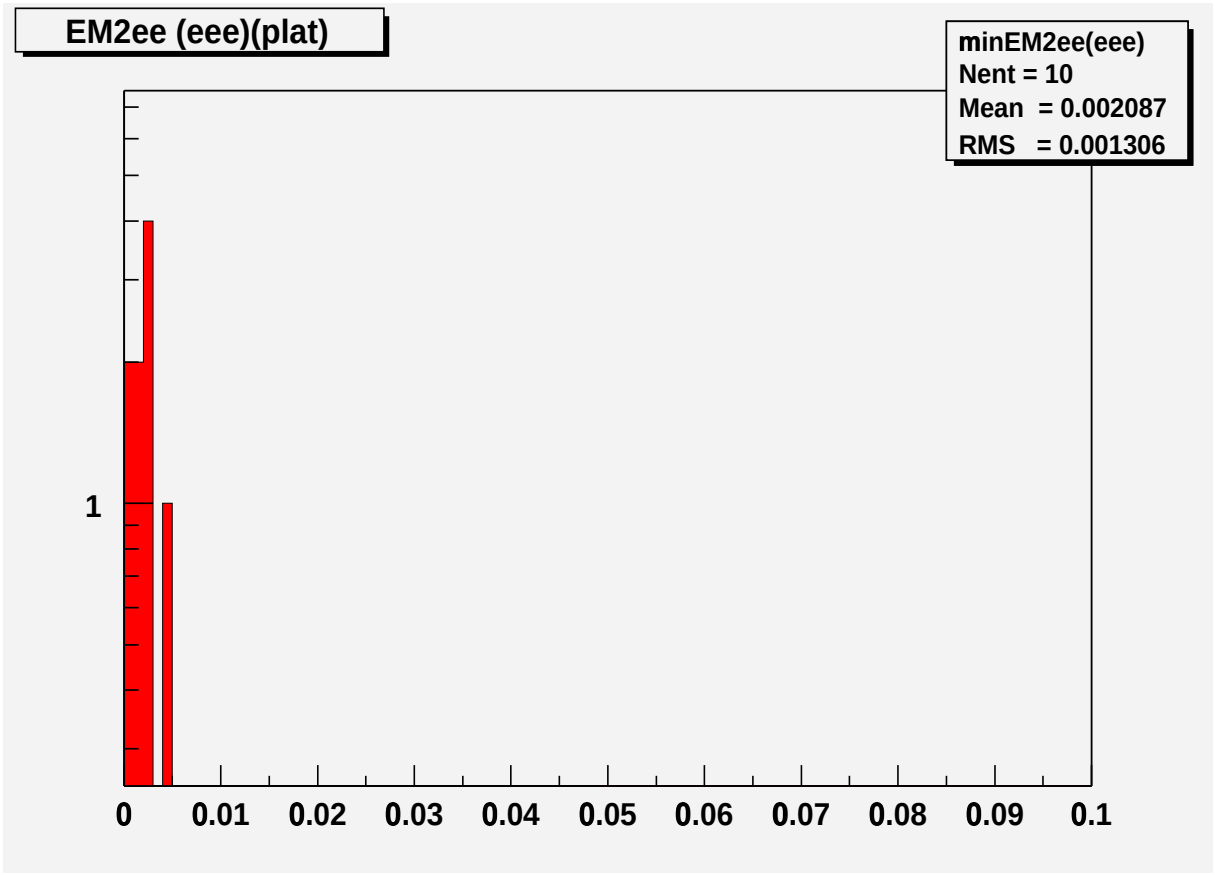

Figure 30: The same as in Fig. 8, but for the eee events.

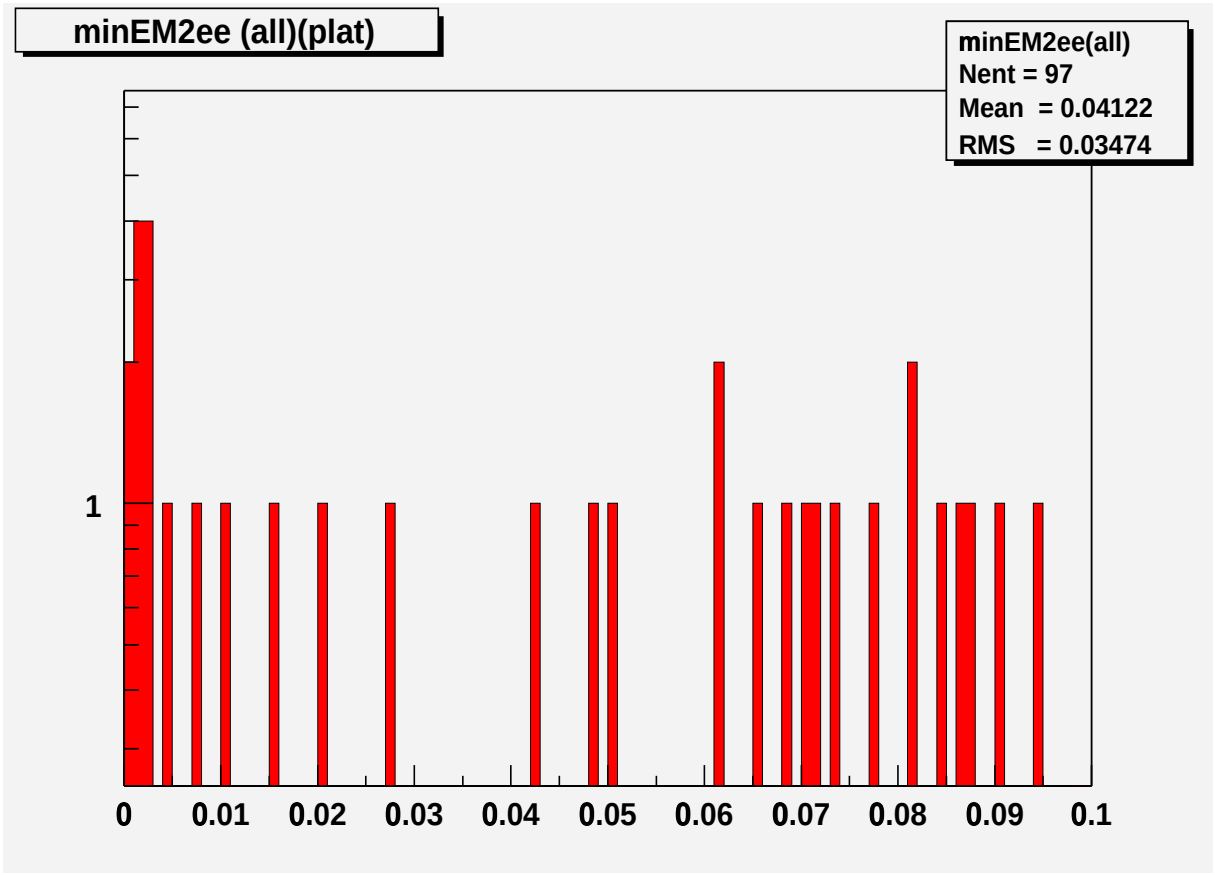

Figure 31: The same as in Fig. 8, but for all "platinum" events.